POST-TRANSLATIONAL MODIFICATION OF FORMATE DEHYDROGENASE, A STRESS-RESPONSE PROTEIN

by

Daryl Robert McNeilly

Submitted in partial fulfillment of the requirements
for the degree of Master of Science

at

Dalhousie University
Halifax, Nova Scotia
April 2016

Table of Contents

LIST OF FIGURES iv
LIST OF TABLES v
ABSTRACT vi
LIST OF ABREVIATIONS USED vii
ACKNOWLEDGMENTS ix
CHAPTER ONE: INTRODUCTION 1
1.1. Ubiquitin Proteasome System 1
1.2. Ubiquitination 1
1.3. 26S Proteasome 3
1.4. Ubiquitin Ligases 5
1.4.1. RING-type E3 Ligases 7
1.5. Keep On Going 7
1.6. Formate Dehydrogenase 8
1.6.1. Changes in FDH Expression in Response to Hormone Treatments 13
1.6.2. Changes in FDH Expression in Response to Environmental Stress 13
1.6.3. Changes in FDH Expression in Response to Exogenous Metabolites 13
1.6.4. Changes in FDH Expression in Response to Biotic Factors 14
1.7. Post-Translational Modification of FDH 14
1.8. Purpose of Study 15
CHAPTER TWO: MATERIALS & METHODS 16
2.1. Plant Materials and Growth Conditions 16
2.2. Plasmids and Cloning 16
2.3. Transient Protein Expression 17
2.4. Protein Extraction and Immunoblot Analysis 17
2.5. Cell-free Degradation Assay 18
2.6. Immunoprecipitation 19
2.7. Ubiquitin Pull Down Assay 20
2.8. Dephosphorylation Assay 20
2.9. Pixel Intensity Analysis 21

2.10. Formate Sensitivity Assay 21
2.11. Sequence Alignment and Post-Translational Modification Prediction 21
2.12. Statistical Analysis 22
2.13. Ubiquitination Assay 23
CHAPTER THREE: RESULTS 24
3.1. FDH is Degraded by the 26S Proteasome 24
3.2. FDH Possesses Multiple Predicted Ubiquitination Sites 24
3.3. Arabidopsis FDH is Ubiquitinated *In Planta* 27
3.4. KEG is Involved in FDH Turnover 32
3.5. A Functional KEG E3 Ligase is Required for FDH Turnover 35
3.6. Arabidopsis FDH is Phosphorylated *In Planta* 35
3.7. KEG Overexpressing Plants are More Tolerant of Formate Stress 39
CHAPTER FOUR: DISCUSSION 43
4.1. Ubiquitination of FDH 43
4.2. KEG Facilitates the Degradation of FDH 43
4.3. FDH Degradation and Formate Sensitivity 44
4.4. Cross Talk between Phosphorylation and Ubiquitination 45
4.5. Model for KEG Regulation of FDH Function 46
4.6. Summary 50
REFERENCES 51
APPENDIX 57

LIST OF FIGURES

Figure 1-1: **The Ubiquitin Proteasome System (UPS)** 2

Figure 1-2: **Outcome of Ubiquitination**……...…….4

Figure 1-3: **The 26S Proteasome**..... 6

Figure 1-4: **KEG Domain Structure**..... 9

Figure 1-5: **KEG And ABA Signalling**…..…….....…10

Figure 1-6: **Interaction Between KEG And FDH**…..……..…...12

Figure 3-1: **FDH is Degraded By The 26S Proteasome**……..……25

Figure 3-2: **Post-Translational Modification Prediction**……...26

Figure 3-3: **Sequence Alignment Matrix**……...28

Figure 3-4: **Ubiquitin Pull-Down Assay**…….31

Figure 3-5: **Ubiquitination Assay**……33

Figure 3-6: **FDH Degradation Is Dependent On KEG**……..34

Figure 3-7: **FDH Degradation Requires A Functional RING Domain**……..36

Figure 3-8: **FDH is Phosphorylated *In Planta***……..40

Figure 3-9: **Dephosphorylation Assay**……...…….41

Figure 3-10: **Formate Sensitivity Analysis**……....42

Figure 4-1: **Model For The Regulation Of FDH By KEG**…….49

Supplemental Figure S-1: **FDH Is Degradaded By The 26S Proteasome**……...57

Supplemental Figure S-2: **FDH Degradation Is Dependent On KEG**…….58

Supplemental Figure S-3: **FDH Degradation Requires A Functional RING Domain**……59

Supplemental Figure S-4: **Dephosphorylation Assay**……...…...…….60

Supplemental Figure S-5: **Formate Sensitivity Analysis**……...…...……...61

Supplemental Figure S-6: **FDH is Phosphorylated *In Planta***……..…..62

Supplemental Figure S-7: **Images of Root Growth**……..63

LIST OF TABLES

Table 1: **Antibodies**……19

Supplemental Table S-8: **Post-translational Modifiction Prediction Score**……64

ABSTRACT

The ability of a plant to adapt to environmental stress is crucial for its ability to grow, develop to maturity and produce yield. The ubiquitination pathway is a post-translational mechanism that aids plants in producing a coping response to stressful conditions such as cold, drought, and pathogen infection. Central to the ubiquitination pathway are the ubiquitin ligases (E3s) that select and mediate attachment of ubiquitin molecules to substrate proteins. A common outcome for tagged proteins is destruction to by the 26S proteasome. The targets of an E3 ligase include proteins involved in many aspects of plant growth, development, hormone signaling, pathogen resistance and tolerance of abiotic stresses. Keep on Going (KEG) is an E3 ligase that negatively regulates the actions of the hormone abscisic acid (ABA) during early seedling establishment. A search for other targets of KEG identified formate dehydrogenase (FDH), which has been previously characterized as a stress response protein. FDH converts formate into carbon dioxide, serving to alleviate any detrimental effects accumulated formate has on the cell. It was of interest to this study to determine if FDH is ubiquitinated and degraded by the 26S proteasome and if KEG is responsible for the regulation of FDH abundance. Results show that FDH is ubiquitinated and phosphorylated *in planta* and that KEG has the capability to attach ubiquitin molecules to FDH *in vivo*. It has also been shown that FDH is being degraded by the 26S proteasome. In addition, *Arabidopsis thaliana* seedlings overexpressing KEG were more sensitive to exogenous formate than their wild-type counter parts. These results suggest that FDH is regulated by KEG, indicating yet another possible role for KEG in modulating plants ability to respond to and cope with environmental stress.

LIST OF ABREVIATIONS USED

cDNA	Complimentary DNA
CFP	Cyan Fluorescent Protein
CIP	Calf-Intestinal Phosphatase
DNA	Deoxyribonucleic acid
E1	Ubiquitin-activating enzyme
E2	Ubiquitin-conjugating enzyme
E3	Ubiquitin Ligase
ECL	Enhanced Chemiluminescence
EDTA	Ethylenediaminetetraacetic acid
EGTA	Ethylene glycol tetraacetic acid
FDH	Formate Dehydrogenase
HA	Hemagglutinin
HEPES	4-(2-hydroxyethyl)-1-piperazineethanesulfonic acid
HERC	Domain homologous to E6 associated protein carboxy-terminus and RCC1 domain protein
IP	Immunoprecipitation
kDa	Kilodalton
KEG	Keep on Going
Lys	Lysine
MES	2-(N-morpholino) ethane sulfonic acid
MG123	26S proteasome inhibitor
mM	Millimolar
OD	Optical Density
PCR	Polymerase Chain Reaction
PVDF	Polyvinylidene fluoride
RING	Really Interesting New Gene

rSAP	Shrimp Alkaline Phosphatase
RT-PCR	Reverse Transcription Polymerase Chain Reaction
SDS	Sodium dodecyl sulfate
SDS-PAGE	Sodium dodecyl sulfate polyacrylamide gel
Ser	Serine
TBS	Tris-Buffered Saline
TBST	Tris-Buffered Saline and Tween 20
Ub	Ubiquitination
UPS	Ubiquitin Proteasome System
WB	Western Blot
μM	Micromolar
β	Beta
α	Alpha
DUB	Deubiquitinating Enzyme
ABA	Abscisic Acid
SA	Salicylic Acid

ACKNOWLEDGMENTS

I wish to express my deepest gratitude to my supervisor Dr. Sophia Stone. She has been an invaluable source of guidance throughout this research project. Her willingness to give her time so generously has been very much appreciated.

I also thank my committee members, Drs. Patrice Côté and Tom MacRae, for their advice at my admissions to candidacy exam and for taking the time to constructively critique my work.

To the past and present member of the Stone lab, in your own ways each of you has been an essential component to the completion of my Master's degree. Thank you Wendy Lyzenga for being a teacher at the lab bench. Thank you to Sarah McVey and Victoria Sullivan for being my lab mates, as well as my friends. You made the troubleshooting process more bearable. Thank you to my loving family for all of your support and encouragement. To my friends in the graduate program, thank you for providing an outlet for my curiosities and opinions. You contributed to filling these last two years full of fond experiences.

CHAPTER ONE: INTRODUCTION

1.1. Ubiquitin Proteasome System

The Ubiquitin Proteasome System (UPS) is an essential pathway in eukaryotic cells that contributes to their normal growth and development by selectively targeting and degrading cellular proteins. Many cellular processes rely the UPS including cell cycle progression, transcriptional regulation, protein signalling and responses to biotic and abiotic stress (Callis and Vierstra, 2000; Hershko et al., 1998; Smalle and Vierstra, 2004). Degradation by the UPS requires that the protein is identified as a target, conjugated with multiple ubiquitin molecules, and then recognized by the 26S proteasome complex (Glickman and Ciechanover, 2002). The importance of the UPS as a regulatory mechanism is evident by its conservation across eukaryotic species (Zuin et al., 2014). For plants, the UPS appears to be particularly significant. Approximately 5% of the *Arabidopsis thaliana* (Arabidopsis) proteome is dedicated to the core components of the UPS (Vierstra, 2003). This significant genomic investment into a single process highlights how important the UPS is to the proper function of eukaryotic cells.

1.2. Ubiquitination

Ubiquitin is a small, heat stable, 8.5 kilodalton (kDa) regulatory protein that is well conserved and present in all known eukaryotes (Callis et al., 1995; Ciehanover et al., 1978). The conservation of ubiquitin is exemplified by the sequence similarity between species. Ubiquitin protein sequences are identical between higher plant species and only differ by three amino acids between human and yeast (Callis et al., 1995; Komander and Rape, 2012). Ubiquitin is attached to a lysine residue of a substrate via the stepwise action of three enzymes (Figure 1-1). The conjugation cascade begins when a ubiquitin molecule is activated in an

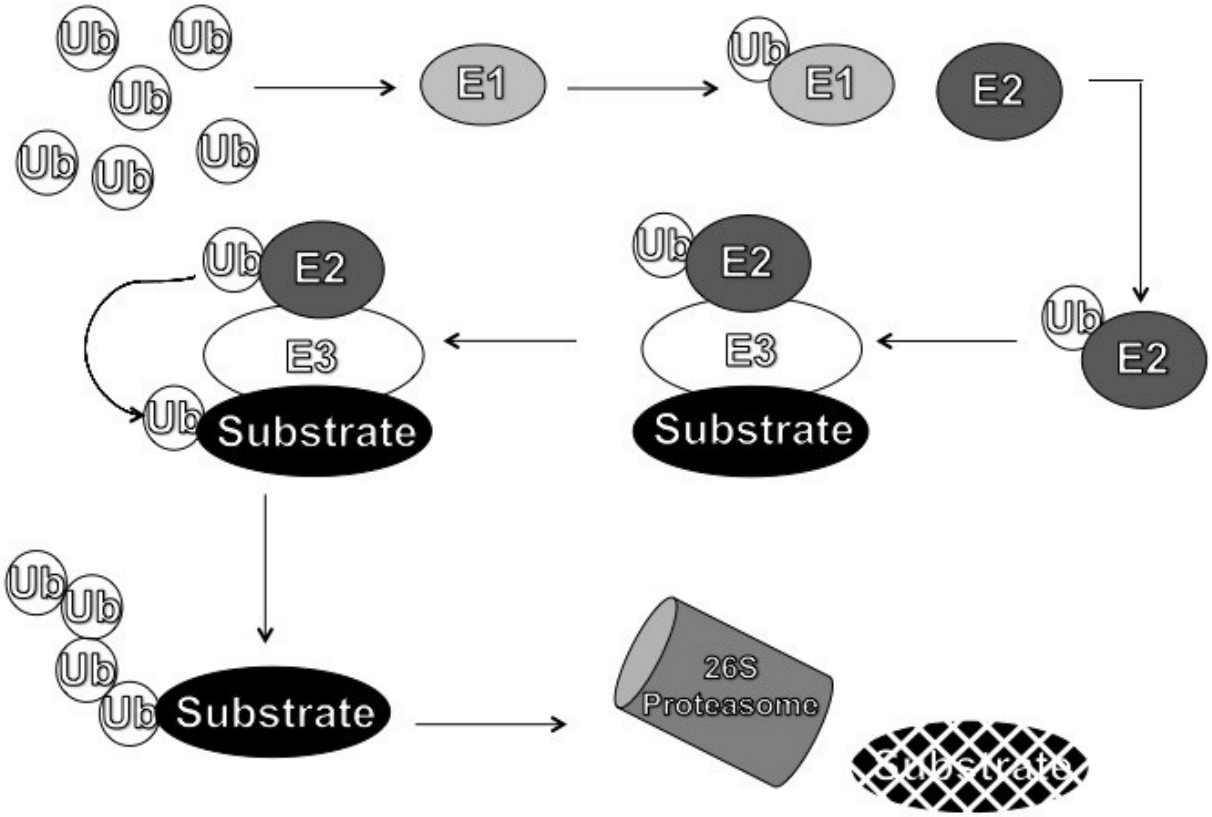

Figure 1-1: The Ubiquitin Proteasome System (UPS). The ubiquitin-activating enzyme (E1) brings ubiquitin (Ub) molecules to the Ub-conjugating enzyme (E2). The Ub-bound E2 then binds to the Ub-ligase (E3) that has already recruited a substrate protein. Here the E3 mediates the transfer of Ub from the E2 onto the substrate. The process is repeated, polyubiquitinating the substrate, which allows it to be recognized by the 26S proteasome, a protease that destroys the polyubiquitinated protein.

ATP-dependant manner by the ubiquitin-activating enzyme (E1). The E1 then transfers the activated ubiquitin molecule to a cysteine residue on the ubiquitin-conjugating enzyme (E2). The E2-Ub intermediate then interacts with the ubiquitin ligase (E3), which recruits a substrate for modification. The E3 facilitates the transfer of ubiquitin from the E2-Ub intermediate onto the substrate in either a direct or indirect manner. For direct transfer, the E3 acts as a scaffold, facilitating the transfer of ubiquitin from the E2 directly onto the substrate. For indirect transfer, the E3 ligase accepts ubiquitin from the E2-Ub intermediate before transferring the regulatory molecule onto the substrate. The type of linkage and number of ubiquitin molecules attached to a protein determines the fate of that substrate. For example, the attachment of one ubiquitin molecule, monoubiquitination, modifies transcription or sends proteins to the lysosome to be turned over (Figure 1-2A) (Smalle and Vierstra, 2004). Multi-monoubiquitination is the attachment of single ubiquitin molecules to different lysine residues on the same protein, resulting in the endocytosis of the modified protein (Figure 1-2B) (Hunter, 2007). If the substrate goes through repetitive rounds of ubiquitination resulting in a chain of ubiquitin molecules on the same lysine residue, then the protein is polyubiquitinated (Figure 1-2C). The most characterized fate of a polyubiquitinated protein is degradation by the 26S proteasome (Figure 1-1).

1.3. 26S Proteasome

The 26S proteasome is a 2.5 Mega Dalton protein complex that is localized in the cytoplasm and nucleus of eukaryotic cells (Peters et al., 1994). The responsibility of this protease complex is to degrade short-lived or damaged proteins. The 26S proteasome is divided into two major sub-complexes, the 20S central core particle (CP) and the 19S regulatory particle (RP) (Vierstra, 2009) (Figure 1-3). The CP is a hollow cylindrical structure composed of four

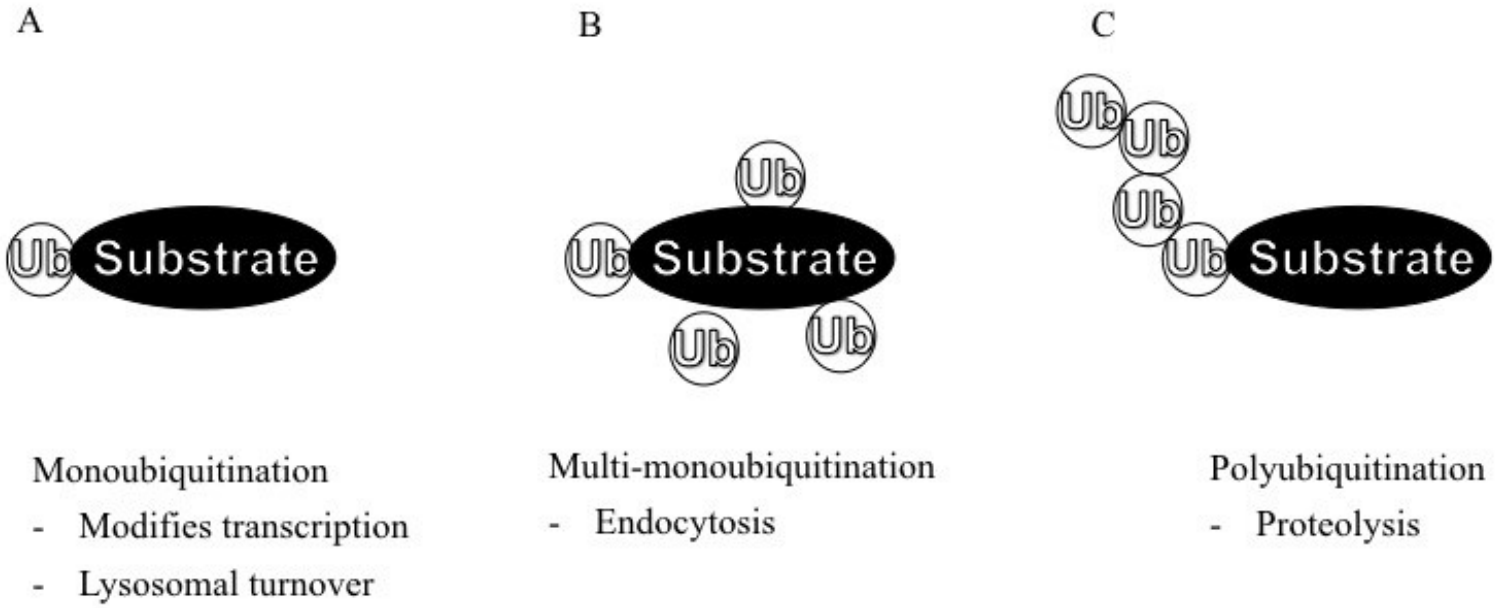

Figure 1-2: Outcomes of Ubiquitination. The post-translational attachment of ubiquitin to a protein determines the fate of that protein in the cell. A) Monoubiquitnation – the attachment of a single ubiquitin molecule to a protein. B) Multi-monoubiquitination – the attachment of several ubiquitin molecules to different lysine residues on the same protein. C) Polyubiquitination – the attachment of multiple ubiquitin molecules in a chain formation anchored to a single lysine residue on a protein.

rings. The outer two rings are each made of seven alpha (α) subunits that act as a physical barrier to the entrance of the hollow channel, while the two inner rings are composed of beta **(**β) subunits that contain protease sites that face the inner cavity (Smalle and Vierstra, 2004). The RP is found on either end of the 20S CP and is subdivided into two complexes, the lid and the base. The base is composed primarily of ATPases that directly interact with the α-subunits of the CP and aid in the unfolding and translocation of target proteins into the hollow channel of the CP (Glickman and Ciechanover, 2002). The lid complex contains ubiquitin receptors that identify proteins conjugated with four ubiquitin moieties as targets for proteolysis (Thrower et al., 2000). In brief, a polyubiquitinated protein is identified by the 19S RP of the 26S proteasome where associated deubiquitinating enzymes (DUBs) remove the ubiquitin molecules to be recycled (Shabek and Ciechanover, 2010). The target protein is then unfolded as it is shuttled into the 20S CP towards the proteolytic sites of the β-subunits (Smalle and Vierstra, 2004). The 26S proteasome cleaves proteins into smaller peptides that are hydrolyzed by downstream proteases into their constituent amino acids so that they are reused (Glickman and Ciechanover, 2002).

1.4. Ubiquitin Ligases

The components of the UPS appear hierarchically in the Arabidopsis genome. There are two genes encoding E1 isoforms (Hatfield et al., 1997), 37 predicted E2 proteins (Kraft et al., 2005) and over 1300 genes encoding E3s and their components (Smalle and Vierstra, 2004). E3 ligases provide the specificity to the UPS by selectively targeting proteins. Since each E3 ligase can have multiple substrates, the large number of E3 ligases encoded results in an even larger number of substrates that can be regulated by the UPS. E3 ligases are categorized by the type of domain used to interact with the E2-Ub intermediate. The three distinct E2-Ub

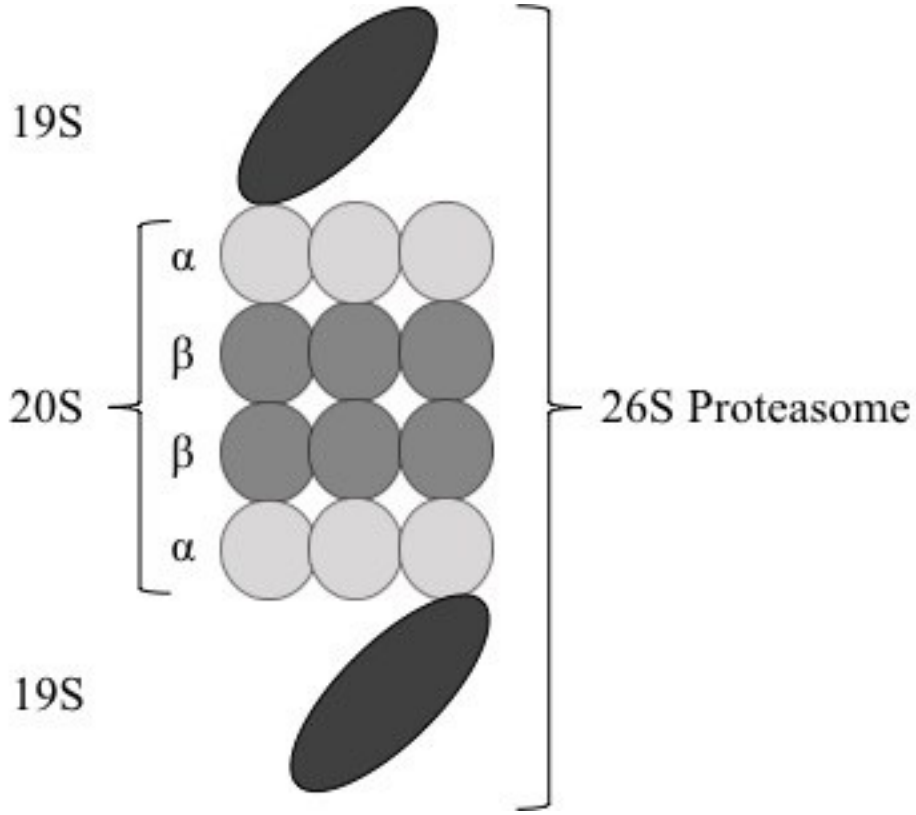

Figure 1-3: The 26S Proteasome. On either end, the 19S regulatory particle (RP) identifies and unfolds lysiene-48 linked polyubiquitinated proteins and translocates them into the 20S core particle (CP). The CP is composed of four hollow stacked rings in the shape of a barrel. The two rings closest to the 19S caps are composed of α-like subunits that act as gates to the central two rings that are composed of β-like subunits housing the proteolytic sites for protein degradation.

interacting domains are the Homology to E6-AP C-terminus (HECT), U-box, and Really Interesting New Gene (RING) domains (Mazzucotelli et al., 2006; Stone, 2014). HECT E3 ligases form an E3-Ub intermediate before donating the ubiquitin molecule to the substrate,whereas RING-type and U-box E3 ligases act as scaffolding, facilitating the direct transfer of ubiquitin onto the substrate directly from the E2 (Smalle and Vierstra, 2004).

1.4.1. RING-type E3 Ligases

The most abundant class of E3 ligases is the Really Interesting New Gene (RING) category. The hallmark of these E3 ligases is a histidine and cysteine rich RING finger motif that binds two zinc atoms forming a cross-braced structure (Borden, 2000; Freemont, 1993). The spacing of the zinc atoms is essential for the structure of the RING domain which is required for interaction with the E2-Ub intermediate, thus contributing to ubiquitination (Pickart, 2001; Zheng et al., 2000). In Arabidopsis, approximately 470 genes are predicted to encode for RING domain-containing proteins (Stone et al., 2005). These RING domain-containing proteins exist as either a monomeric E3 or as a part of a multimeric ubiquitin ligase which respectively have the E2-Ub and substrate binding domains on the same protein or on separate proteins in a complex (Deshaies and Joazeiro, 2009).

1.5. Keep On Going

Keep on Going (KEG) is an example of a well-studied monomeric RING-type E3 ligase found in Arabidopsis. KEG has a unique domain organization because in addition to the characteristic RING domain, it also has a kinase domain, as well as Ankyrin and HERC repeats that provide sites for substrate interaction and cellular localization (Figure 1-4) (Gu and Innes, 2011; Sedgwick and Smerdon, 1999; Stone et al., 2006). Homologs of *KEG* are found in other plant species such as O*ryza sativa* (rice), *Medicago truncatula* (barrelclover*),*

and *Populus tricocarpa* (California poplar) (Stone, 2006). KEG is of great interest because of its involvement in the regulation of plant hormones, specifically Abscisic Acid (ABA). Phytohormones, such as ABA, are involved in many plant processes that favour the production of viable offspring. After germination, ABA synthesis and cellular accumulation of the hormone increase in response to various abiotic factors, including drought, heat/chilling and salt stress (Swamy and Smith, 1999). The increase in ABA abundance signals for protective responses, such as delayed growth, which provides a coping mechanism allowing plants to tolerate the environmental strain exerted by abiotic stresses (Brocard, 2002). Using the UPS pathway, KEG ensures that in the absence of abiotic stress, ABA signalling is inhibited, allowing young seedlings to become established (Stone et al., 2006). KEG does this by ubiquitinating components of the ABA signalling network, including Calcineurin B-Like Interacting Protein Kinase (CIPK) 26 and Abscisic acid Insensitive (ABI) 5, responsible for regulating the expression of ABA-responsive genes, by mediating their destruction via the 26S proteasome (Figure 1-5) (Liu and Stone, 2010; Lyzenga et al., 2013; Stone et al., 2006). By regulating CIPK26 and ABI5 abundance KEG ensures that only stress-induced accumulation of ABA can trigger hormone mediated coping mechanisms. The involvement of KEG in ABA signalling is dependent on the E3 ligase's interaction with multiple ABA dependent transcription factors as characterized by various studies (Liu and Stone, 2010; Chen et al., 2013; Lyzenga et al., 2013).

1.6. Formate Dehydrogenase

A Yeast-two Hybrid (Y2H) analysis identified a potential KEG interacting protein, formate dehydrogenase (FDH) (Figure 1-6A) (Schofield, unpublished). The Y2H results were

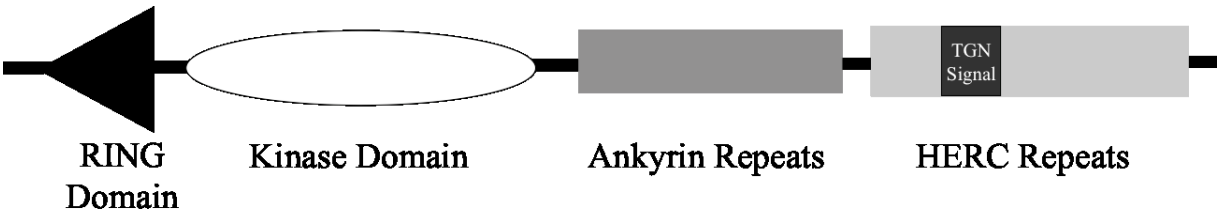

Figure 1-4: KEG Domain Structure. Simplified KEG structure adapted from Stone et al., 2006. KEG possesses a unique domain organization that includes the RING domain, responsible for binding E2-Ub intermediates, a kinase domain, capable of phosphorylation, as well as ankyrin and HERC repeats that facilitate protein-protein interaction and the localization of KEG. The fifth HERC repeat is involved in localizing KEG to the trans-Golgi network (TGN).

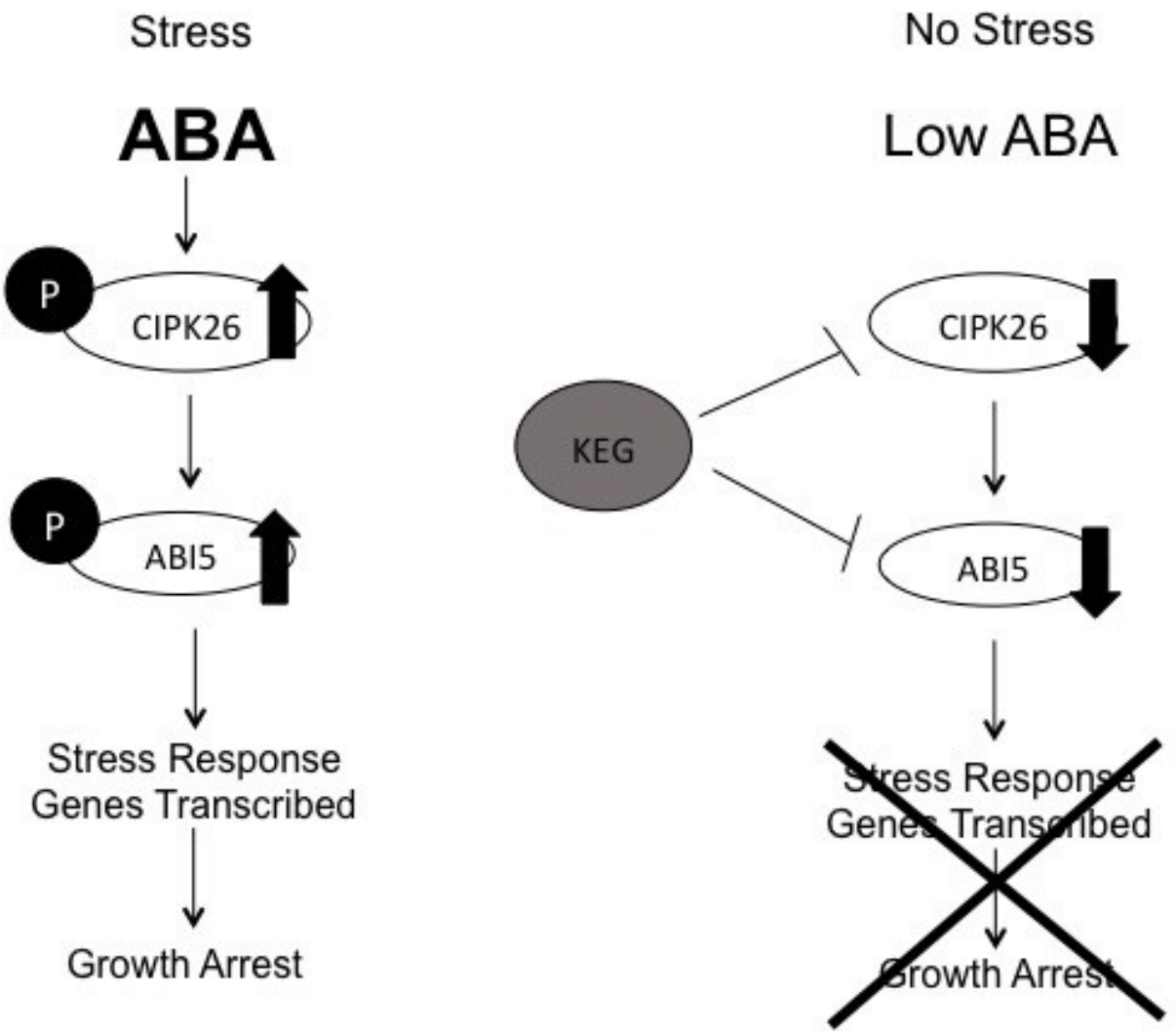

Figure 1-5: KEG And ABA Signalling. Simplified representation of the role KEG plays in ABA signaling – In the presence of a stress, abscisic acid (ABA) accumulates in the cell and leads to the activation of protein kinases, like Calcineurin B-Like Interacting Protein Kinase (CIPK) 26, and transcription factors, like Abscisic acid Insensitive (ABI) 5 transcription factor, through their phosphorylation, promoting protective stress responses. In the absence of stress, ABA levels are low, so the RING-type E3 ligase, Keep on Going (KEG) inhibits both CIPK26 and ABI5 by targeting them for ubiquitination and subsequent degradation by the 26S proteasome.

confirmed with a Glutathione S-transferase (GST) pulldown assay (Figure 1-6B) which showed that the HERC domain of KEG interacts with FDH (Schofield, unpublished). FDH is an enzyme responsible for catalyzing the redox reaction that oxidizes formate ions into carbon dioxide, while reducing NAD+ to NADH (Popov, 1994). Formate is a toxic compound, inhibiting cellular respiration and root growth in Arabidopsis (David et al., 2010; Li et al., 2002). As such, FDH's role in plants has previously been suggested to be formate detoxification (Li et al., 2002). The FDH that interacts with KEG is classified as an NAD+ dependent FDH because of its reliance on NAD as a co-factor, and it is found in bacteria, methalotrophic yeasts, plants and mammals (Hourton-Cabassa et al., 1998).

The expression of FDH varies among plant species and between tissue types. Studies conducted with *Solanum tuberosum* (potato) and *Capsicum annuum* (pepper) have shown that *FDH* mRNA and protein are the most abundant in developing tubers and flowers, respectively, while least abundant in leaf tissue (Choi et al., 2014; Hourton-Cabassa et al., 1998). In Arabidopsis, *FDH* expression is similar in leaf, stem and flower tissue, while the lowest is seen in the roots (Li et al., 2001). In leaf tissues, FDH localizes to mitochondria (Oliver, 1981) and potentially to chloroplasts (Olson et al., 2000). The expression of *FDH* is drastically increased when healthy plant tissue is subjected to stressful conditions such as hypoxia, drought, wounding, chilling, heat, iron-deficiency and pathogen infection, suggesting that FDH is involved in stress response (Choi et al., 2014; Colas des Francs-Small et al., 1993; Hourton-Cabassa et al., 1998; Li et al., 2001; Suzuki et al., 1998)

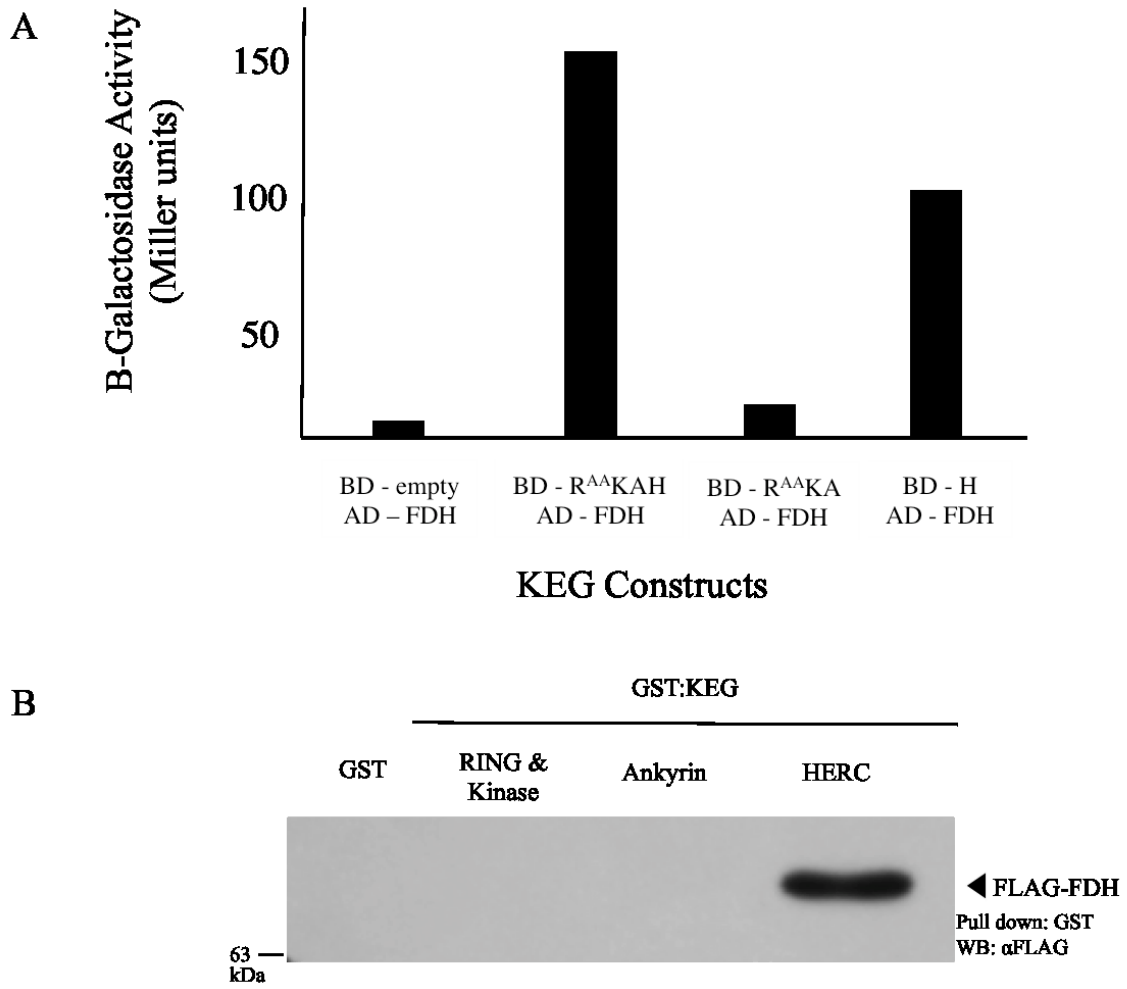

Figure 1-6: Interaction Between KEG and FDH. A) Yeast two-hybrid analysis showing interaction between KEG and FDH. The activation of the downstream reporter gene encoding β-Galactosidase is dependent on a transcription factor binding to an upstream activating sequence. The transcription factor is split into two halves, a binding domain (BD) and an activating domain (AD). Fusion of the BD and AD to proteins that interact allows for the reconstitution of the transcription factor and promotes the expression of the reporter gene. β-Galactosidase hydrolyzes the compound X-gal, supplemented in the growth medium, creating a blue signal. The higher the signal the stronger the interaction between proteins. The BD was used either as an empty control or it was fused to KEG. FDH is fused to the activating domain (AD) in each experiment. R, K, A and H, represent the RING, Kinase, Ankyrin and HERC domains of KEG, respectively. R^{AA} is a mutated version of the RING domain intended to prevent the ubiquitination and degradation of FDH during the assay. Note that FDH binds to the full length KEG (R^{AA}KAH) and has a high affinity for the HERC (H) domain (Schofield, unpublished). B) Glutathione S-transferase (GST) pull-down assay using bead-bound GST, GST-RING&Kinase, GST-Ankyrin or GST-HERC and bacterial cell lysates containing FLAG-FDH. Note that GST-HERC was able to pull down FLAG-FDH from bacterial lysates as detected by western blot (WB) analysis with FLAG antibodies (Schofield, unpublished)

1.6.1. Changes in FDH Expression in Response to Hormone Treatments

Plant hormones are structurally simple molecules that are involved in regulating all known aspects of plant growth and development (Wang and Irving, 2011). Additionally, in unfavourable growing conditions, plant hormones serve as signals to initiate coping responses. For example, in drought conditions, ABA is synthesized and promotes stomata closure to reduce the amount of water lost to transpiration (Jones and Mansfield, 1970).

Exogenous treatment with plant hormones simulates the perception of external stresses, triggering a coping response by promoting the expression of stress response genes. Application of three plant hormones, ABA, salicylic acid (SA), and ethylene each increases the amount of *FDH* mRNA in leaf tissues of potato, pepper, and Arabidopsis plants (Choi et al., 2014; Hourton-Cabassa et al., 1998; Li et al., 2001). The hormonal induction of *FDH* expression indicates that the enzyme is involved in stress related coping responses.

1.6.2. Changes in *FDH* Expression in Response to Environmental Stress

A plant's inability to relocate when environmental conditions become unfavourable has led to the evolution of an arsenal of coping responses that are under the control of a variety of plant hormones. Exposure to adverse environmental conditions triggers a stress response facilitated by the up-regulation of various stress response genes. In potato, *FDH* mRNA increases in leaf tissue when cold, drought, dark and aerobic conditions are simulated (Hourton-Cabassa et al., 1998). A similar expression pattern of *FDH* was observed in barely under anaerobic and iron-deficient conditions (Suzuki et al., 1998)

1.6.3. Changes in *FDH* Expression in Response to Exogenous Metabolites

It has been previously suggested that FDH is involved in the metabolism of one-carbon compounds (C1-compounds), such as formate (Li et al., 2003). These compounds are essential

for the synthesis of folate and amino acids (Hanson and Roje, 2001) *FDH* is up-regulated in tissues treated with various C1-compounds has been observed. For example, application of formate, formaldehyde or methanol to potato leaves increases the expression of *FDH* (Hourton-Cabassa et al., 1998).

1.6.4. Changes in *FDH* Expression in Response to Biotic Factors

Similar to abiotic stresses, *FDH* expression is induced in leaf tissue by pathogen infection. In pepper plants, both virulent and avirulent infection with *Xanthomonas campestris pv vesicatoria* induces the expression of *FDH*; the latter showing a more pronounced induction (Choi et al., 2014). FDH is required for the induction of the hypersensitive cell death response by up-regulating the expression of genes encoding defence-related proteins and the synthesis of the defense hormone, SA. Comparable results were found in Arabidopsis infected with *Pseudomonas syringae* pv tomato DC3000. *FDH* gain-of-function transgenic plants showed an increase in SA levels and expression of defensive proteins (Pathogenesis-Related 1 and 4), which inhibited *Pseudomonas syringae pv tomato* DC3000 growth more effectively than did the loss-of-function *FDH* mutants (Choi et al., 2014).

1.7. Post-Translational Modification of FDH

Proteins are modified in various ways, including phosphorylation. The addition of a phosphoryl group to serine, threonine or tyrosine residues is associated with the activation, deactivation or alteration of enzymatic function. For example, the phosphorylation of the mammalian nuclear protein, p27, results in its nuclear export (Besson et al., 2006). Phosphorylation induced conformational change in protein structure plays a central role in cellular processes such as signal transduction (Graves and Krebs, 1960), cell cycle regulation (Gu et al., 1992), and protein-protein interactions (Nishi et al., 2011). The importance of

phosphorylation as a regulatory mechanism is demonstrated by the observation that it is one of the most commonly observed post-translational modifications (Khoury et al., 2011).

FDH in potato is phosphorylated at two threonine (T) residues, T76 and T333, a modification strongly reduced by the presence of formate (Bykova et al., 2003). Mass spectrometry of proteins from Arabidopsis tissue has identified two serine (S) residues, S15 and S16 as phosphorylated residues (Roitinger et al., 2015). In a separate study, the treatment of Arabidopsis with ABA and mannitol revealed that only the S15 residue was phosphorylated (Xue et al., 2013). In both potato and Arabidopsis, the phosphorylation level of FDH decreases when stress-related metabolites or hormones are present.

1.8. Purpose of Study

FDH has been characterized as a stress response protein for about three decades. The diverse set of conditions that induce *FDH* expression suggests that the enzyme plays an important role in various stress responses. FDH interaction with KEG suggests regulation of the enzyme by the UPS. Studying the interaction between KEG and FDH will provide insight into regulation of this important yet poorly understood stress protein. The aims of this study are to: 1) determine if FDH is ubiquitinated and degraded by the 26S proteasome; 2) establish if KEG is involved in targeting FDH for degradation by the 26S proteasome; 3) investigate the phosphorylation state of FDH and how it contributes to the proteins stability 4) provide further evidence for a functional connection between FDH and KEG by determining if there is a role for KEG in response of plants to formate stress.

CHAPTER TWO: MATERIALS & METHODS

2.1. Plant Materials and Growth Conditions

Arabidopsis thaliana ecotype Columbia (Col-0) and transgenic seeds were surface-sterilized with 50% (v/v) bleach and 0.1% Triton X-100 for ten minutes at room temperature. After cold treatment at 4°C for 2 days, seeds were germinated and grown on solid ½ Murashige and Skoog (MS) medium containing 0.8% agar and 1% sucrose under continuous light at 22°C. For plants grown in soil, 7-day-old seedlings were transferred from solid ½ MS medium to soil and grown under photoperiodic cycles of 16 hours light and 8 hours dark at 22°C in a growth chamber (Sparkes et al., 2006). *Nicotiana benthamiana* (tobacco) plants were germinated on soil, transferred to individual pots, and grown under the same phototropic period as described above.

2.2. Plasmids and Cloning

Previously, the full-length cDNAs of *FDH* (At5g14780) and *KEG* (At5G13530) were obtained by reverse transcription (RT)-PCR using SuperScript II reverse transcriptase (Invitorogen) (Schofield et al, unpublished; Liu and Stone, 2010) and introduced into the Gateway ® entry vector pDONR201 (Invitrogen) as per manufacturer's instructions. Point mutations were introduced with the Phusion site-directed mutagenesis kit (Finnzymes) to create a mutated RING (R^{AA}) domain in *KEG* (C-29-A, H-31-A; KEG^{AA}). Nucleotide sequences were confirmed by DNA sequencing (McGill University and Génome Québec Innovation Centre). *FDH*, *KEG* and KEG^{AA} cDNAs in their individual entry vectors, pDONR201, were introduced into pEarleyGate102 or pEarleyGate201 plant transformation vectors (Earley et al., 2006). FDH was produced as an in-frame fusion with the cyan fluorescence protein (CFP) and hemagglutinin (HA) tag (CFP-HA-FDH) while KEG/KEG^{AA}

was fused to the HA tag (HA-KEG/HA-KEG^{AA}). Expression of all transgenes was under the control of the constitutive cauliflower mosaic virus 35S promoter.

2.3. Transient Protein Expression

Following Sparkes et al., 2006, *Agrobacterium tumefaciens* GV3101 (Agrobacterium) were transformed with the plant transformation vectors, pEarleyGate102 or pEarleyGate201 containing the coding region for *FDH* (*35S:CFP-HA-FDH*) or *KEG/KEG^{AA}* (*35S:HA-KEG* or *35S:HA-KEG^{AA}*), respectively. Agrobacterium cultures were collected and then resuspended in an infiltration solution containing 5 mg/ml D-glucose, 50 mM MES, 2 mM Na_3PO_4, and 0.1 mM acetosyringone. The resulting bacterial suspensions were adjusted with additional infiltration solution to an optical density (OD) of $OD_{600} \approx 0.8$. For co-infiltration, Agrobacterium suspensions transformed with *35S:HA-KEG* or *35S:HA-KEG^{AA}* and *35S:CFP-HA-FDH* were mixed in a 50:50 ratio. A needleless syringe was used to introduce the Agrobacterium suspensions into the underside of leaves of six-week-old tobacco plants. Infiltrated tobacco leaves were collected after 48 hours for protein extraction and stored at -80°C. Immunoblot analysis (described below) using antibodies that recognize HA were used to confirm expression of the fusion proteins in infiltrated tobacco tissue.

2.4. Protein Extraction and Immunoblot Analysis

Protein extracts were obtained by homogenizing infiltrated tobacco tissue in a standard protein extraction buffer consisting of 20mM Tris HCl (pH 7.5), 100mM NaCl, 1mM EDTA, 1mM EGTA, 1mM phenylmethylsulfonyl fluoride (PMSF), 10mM dithiothreitol (DTT), 30µM Z-Leu-Leu-Leu-al (MG132), 6% glycerol, and protease inhibitor cocktail (Sigma-Aldrich). Homogenized samples were centrifuged for 5 minutes at 14,000 g to pellet any debris. Supernatant was transferred to a fresh eppendorf tube and centrifuged again to pellet

any remaining debris. To each sample 6x Sodium dodecyl sulfate (SDS) loading buffer (300 mM Tris-HCl pH 6.8, 30% glycerol, 12% SDS, 5% β-mercaptoethanol, 0.6% Bromophenol Blue) was added before being placed in a boiling water bath for 5 minutes followed by centrifugation at 10 000 g for 3 minutes. Denatured samples were loaded in a 7.5% SDS polyacrylamide separating gel (SDS-PAGE) topped with a 5% SDS-PAGE stacking gel. All SDS-PAGE used the Tris-Glycine Laemmli buffer system (Laemmli, 1970). Proteins were separated by gel electrophoresis within the SDS-PAGE. Proteins were then transferred from the polyacrylamide gel to polyvinylidene fluoride (PVDF) membrane using a semi-dry electo-transfer unit. Following protein transfer, the PVDF membrane was blocked with 5% milk solution and Tris-buffered saline (TBST) (50 mM Tris-HCl, pH7.5, 150 mM NaCl and 0.05% Tween 20) for 1 hour at room temperature. PVDF was then incubated with primary antibody for 1 hour, followed by three 10-minute washes with TBST. Secondary antibody was added for 1 hour, followed by an additional three 10-minute washes with TBST. Antibodies used in the incubations were specific to the tags fused to the proteins of interest (Table 1). Proteins of interest were then visualized on light sensitive film using an Enhanced Chemiluminescence (ECL) Western Blotting Substrate kit as per manufacturer's instructions (Thermo Scientific). Ponceau S was used to stain PVDF membranes after western blotting to show protein loading.

2.5. Cell-free Degradation Assay

Cell free degradation assays were carried out as previously described (Wang et al., 2009). Briefly, total protein extracted from tobacco tissue expressing CFP-HA-FDH alone or co-expressing HA-KEG/ HA-KEG^{AA} was incubated at 25°C with 10mM adenosine triphosphate (ATP). Equal volumes of each reaction were removed at the indicated time points and 6x SDS loading buffer was added to stop the reaction. For assays with the 26S

Table 1: Antibodies. List of primary and secondary antibodies used to detect HA-fusion proteins in immunoblot analysis and phosphorylated serine residues.

Protein Tag	Primary Antibody	Secondary Antibody	Dilution Factor
Heamagluttinin (HA)	Mouse anti-HA (Sigma-Aldrich)	Anti-Mouse (Sigma-Aldrich)	1:5000
Phosphate	Phosphoserine	Anti-Rabbit IgG (Sigma-Aldrich)	1:1000

proteasome inhibitor, MG132, total protein extract was divided equally into two treatments. One treatment was supplemented with 30μM MG132 while the other received an equivalent volume of extraction buffer. The reaction mixtures were incubated for 30 minutes at 25°C before the addition of 10mM adenosine triphosphate, which marked time point zero. Equal volumes of each reaction mixture were removed at the indicated time points and 6x SDS loading buffer was added to stop the reaction. All samples were loaded into SDS-PAGE gels, subjected to immunoblot analysis as described above.

2.6. Immunoprecipitation

Protein extracts were prepared from tobacco tissue expressing CFP-HA-FDH using the following buffer: 50mM HEPES (pH 7.5), 5mM EDTA (pH 8), 5mM EGTA (pH 8), 10mM Na_3VO_4, 10mM NaF, 25mM β-glycerophosphate, 1mM phenylmethylsulfonyl fluoride, 5% glycerol, 30μM MG132 and protease inhibitor cocktail (Sigma-Aldrich). EZview Red HA-Agarose beads (Sigma-Aldrich), prepared according to manufacturers instructions, were added to protein extracts and incubated at 4°C for 4 hours. After incubation, HA-beads were collected by centrifugation at 18 000g for 30 seconds, followed by two washes with TBS (50 mM Tris-HCl, pH7.5, 150 mM NaCl). Washed HA-beads were either used for elution or

immediately mixed with 30µL of 1X SDS, boiled for 5 minutes, centrifuged at 10 000g for 3 minutes then loaded onto SDS-PAGE gels, followed by immunoblot analysis, as previously described.

For elution of CFP-HA-FDH proteins, HA-beads were mixed continually in 0.2M glycine (pH 2) buffer for 10 minutes followed by centrifugation at 18 000g for 30 seconds. The resulting supernatant was neutralized by adding an equal volume of 1M Tris (pH 8.0). To determine the success of the elution protocol, samples were mixed with 6X SDS loading buffer, loaded onto SDS-PAGE gels and subjected to immunoblot analysis (Table 1) to visualize CFP-HA-FDH.

2.7. Ubiquitin Pull Down Assay

Following the procedure of Kong *et al.*, 2015 total protein extract from tobacco tissue transiently expressing CFP-HA-FDH was incubated for 4 hours at 4°C with 25µL of p62-agarose (Enzo Life Science) beads that were prewashed twice in 500µL TBST. Total protein extract was prepared using 50mM Tris HCl (pH 7.5), 20mM NaCl, 1mM PMSF and 50µM MG132. After incubation, the p62-agarose beads were washed twice with an initial wash buffer (Tris HCl (pH 7.5), 20mM NaCl) followed by one additional wash with a final wash buffer (Tris HCl (pH 7.5), 200mM NaCl). Samples received 25µL 1xSDS loading buffer before being placed in a boiling water bath, then were centrifuged and separated by an SDS-PAGE gel and subjected to immunoblot analysis with the HA antibodies (Table 1) specific to CFP-HA-FDH. Pull-down results are representative of a single trial.

2.8. Dephosphorylation Assay

Total protein extracts from tobacco tissue transiently expressing CFP-HA-FDH and un-infiltrated tobacco tissue (control) were subjected to a Bradford (Sigma-Aldrich) assay, as per

manufacturers instructions, to determine and equalize the total protein concentrations. 50µg of total protein extract containing CFP-HA-FDH were equally split into two treatments. One treatment was supplemented with a shrimp alkaline phosphatase (rSAP; Sigma) while the other received an equal volume of protein extraction buffer to account for volumetric differences between the reactions. The samples were incubated at 37°C for one hour and then subjected to SDS-PAGE and immunoblot analysis with an HA antibody (Table 1).

2.9. Pixel Intensity Analysis

Western blots that required the quantification of protein bands were loaded into the image analysis program Image J (http://imagej.nih.gov/ij/; Abràmoff et al., 2005) and the mean pixel intensity for each band was quantified using the 16-bit grey scale, where 0 is absolute black and 255 is absolute white. For ease of interpretation, the pixel intensity values represented were inverted to give the darker pixels a higher score and lighter pixels a lower score.

2.10. Formate Sensitivity Assay

As described by Li et al, 2002 wild type and transgenic Arabidopsis plants (35S:*HA-KEG)* constitutively expressing *HA-KEG* were grown on solid ½ MS medium for seven days before being transferred to solid ½ MS medium either supplemented with 0.4 mM sodium formate or unsupplemented (0mM sodium formate). At 24-hour intervals the length of the primary root was measured from the point of transfer to the treatment plates and an average for each genotype was calculated. Two independent trials were conducted using 6 plants per genotype per trial for a total of 12 plants. Representative photographs of the root growth are available in the appendix (Supplementary Figure S-7).

2.11. Sequence Alignment and Post-Translational Modification Prediction

FDH protein sequences for *Solanum lycopersicum* (tomato-Accession NP_001234857),

Oryza sativa Japonica (rice-Accession XP_015642621.1), *Glycine max* (soybean-Accession NP_001241141.1), *Vitis vinifera* (grape-Accession XP_002278444.1), *Brachypodium distachyon* (stiff brome-Accession XP_003563874), *Sorghum bicolor* (sorhgum-Accession XP_002438408), *Populus trichocarpa* (poplar-Accession XP_002320501.1), *Selaginella moellendorffii* (Accession XP_002985142), *Hordeum vulgare* (barley-accession BAJ95739.1), *Solanum tuberosum* (potato-Accession NP_001274827.1) were collected from the NCBI UniGene data base (http://www.ncbi.nlm.nih.gov/unigene), *Capsicum annuum* (sweet pepper) protein sequence was obtained from Choi et al., 2014, and the *Arabidopsis thaliana* (AT5g14780) protein sequence was obtained from The Arabidopsis Information Resource (TAIR). Sequences were converted to FASTA format and introduced into The European Bioinformatics Institutes (EBI) Clustal Omega protein sequence alignment program (McWilliam et al., 2013).

For post-translational modification predications, the protein sequence for Arabidopsis FDH was input into Ubiprober (http://bioinfo.ncu.edu.cn/UbiProber.aspx) (Chen et al., 2013) and NetPhos 2.0 (http://www.cbs.dtu.dk/services/NetPhos/) (Blom et al., 1999) to identify potential ubiquitination and phosphorylation sites, respectively.

2.12. Statistical Analysis

A pooled Students t-test was performed to discern if the differences in average root length between +/- formate treatments were significant. An unpooled test was used when the standard deviations of the independent means were not similar to one another (Welch, 1947). Independent means were compared; t-test statistics and degrees of freedom were used to determine the p-value. For the purpose of this study, the criteria for statistical significance were set at a Type I error rate of 5%.

2.13. Ubiquitination Assay

RING mutant *KEG* (*KEG*^{AA}) was expressed as His-GST fusion, FDH was expressed as a Flag-His tagged fusion, and Arabidopsis UBC8 was expressed as a His-tagged fusion protein. All proteins were expressed in *Escherichia coli* strain Rosetta (DE3) and purified using nickle-charged resin (Bio-Rad) according to the manufacturer's instructions. The assay was performed as previously described (Stone et al., 2006). Briefly, reactions containing 50mM Tris-HCl, pH 7.5, 10 mM MgCl2, 0.05 mM ZnCl2, 1 mM ATP (Sigma- Aldrich), 0.2mMDTT, 10mM phosphocreatine, 0.1 unit of creatine kinase (Sigma-Aldrich), 50 ng of yeast E1 (BostonBiochem), 150 ng of purified His-AtUBC8 (E2), 2 mg of ubiquitin (BostonBiochem), 300 ng His-GST-KEG^{AA} (RING mutant), and/or 300 ng Flag-His-FDH were incubated at 30°C for 2 h. Reactions were stopped by adding SDS sample buffer and analyzed by SDS-PAGE followed by immunoblot analysis with antibodies that recognized the His tag.

CHAPTER THREE: RESULTS

3.1. FDH is Degraded by the 26S Proteasome

The interaction between FDH and KEG, as observed in the Y2H and GST pull-down, indicates that the UPS may regulate FDH abundance (Schofield, unpublished). In order to determine if the UPS targets FDH for degradation, transiently transformed tobacco tissue expressing *CFP-HA-FDH* was used in cell free degradation assays with or without the 26S proteasome inhibitor, MG132. If FDH is turned over by the 26S proteasome then the addition of MG132 to the assay should impede its degradation, resulting in greater FDH stability. In the absence of MG132, CFP-HA-FDH gradually disappeared from the protein samples analyzed over time (Figure 3-1B and Supplemental Figure S-1). In contrast, when MG132 was included in the assay the abundance of CFP-HA-FDH was more stable over time (Figure 3-1A). The graph in figure 3-1C, shows the average difference in FDH abundance over time in the presence and absence of the proteasome inhibitor from two separate assays. The slower degradation rate of CFP-HA-FDH in the presence of MG132 suggests that FDH is a substrate for the 26S proteasome.

3.2. FDH Possesses Multiple Predicted Ubiquitination Sites

Since the degradation of a protein by the 26S proteasome is typically preceded by ubiquitination, it was worthwhile to investigate the extent to which FDH is be ubiquitinated. To explore the potential for Arabidopsis FDH ubiquitination, the protein sequence of the enzyme was analyzed using an ubiquitination site prediction program (Chen et al., 2013a). The prediction software identified nine lysine (K) residues that could be ubiquitinated (Figure 3-2 and Supplementary Table S-8), indicating that the modification of FDH for targeting to the 26S proteasome was possible.

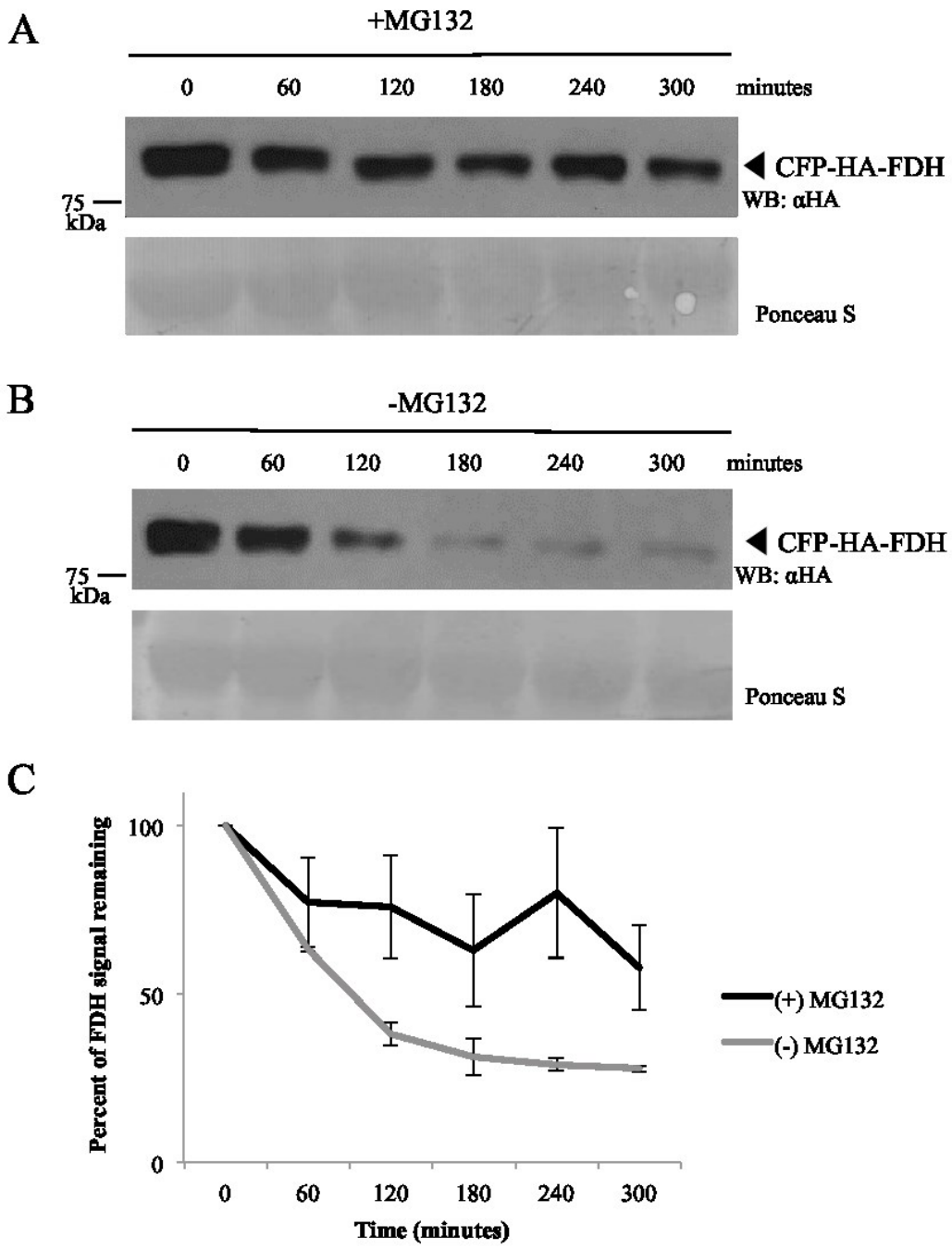

Figure 3-1: FDH Is Degraded By The 26S Proteasome. Reprsentative Cell free degradation assay using tobacco tissue transiently expressing CFP-HA-FDH. Protein extract was divided equally into two treatments. A) Received the 26S proteasome inhibitor, MG132, while B) received no additional supplements. Equal volumes were removed from each treatment at the indicated time points to observe the abundance of CFP-HA-FDH over time. Protein samples were subjected to SDS-PAGE and immunoblot analysis with antibodies that recognize HA. C) Average pixel intensity of CFP-HA-FDH protein bands from the representative and replicated cell free degradation assays showing the percent of FDH remaining over time. Bars represent the standard error of mean (n=2). Ponceau S shows the protein loading in each lane.

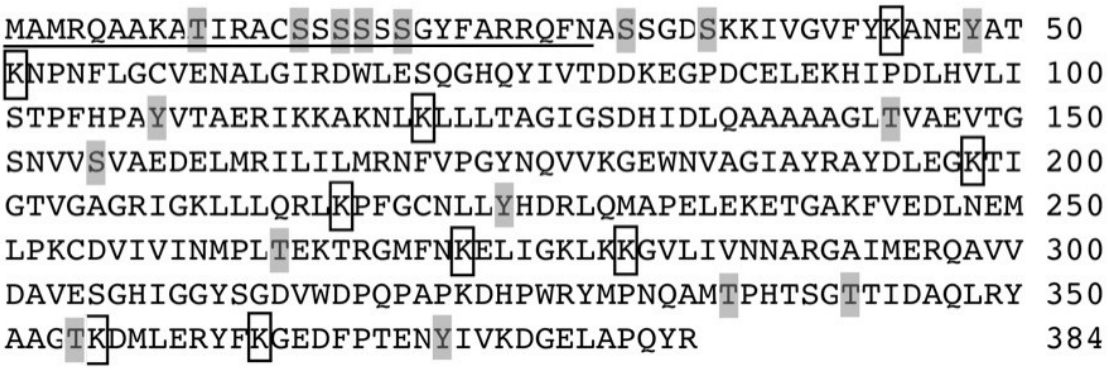

Figure 3-2: Post-Translational Modification Predictions. Arabidopsis FDH (At5g14780) protein sequence with predicted ubiquitination (Chen et al., 2013a) and phosphorylation (Blom et al., 1999) sites highlighted. Nine lysine (K) residues (black outline) are potential ubiquitination sites while seven serine (S), six threonine (T) and four tyrosine (Y) residues are predicted to be sites of phosphorylation (grey boxes). Underlined amino acids represent predicted mitochondrial targeting sequence (Herman et al., 2002).

To determine if the predicted ubiquitination sites in Arabidopsis FDH are found in other organisms, an alignment of FDH protein sequences from 11 other plant species was conducted to determine if they share predicted ubiquitination sites.. Of the nine predicted ubiquitination sites mentioned above, K199, K217 and K273 were conserved between all 12 species (Figure 3-3A). Of the remaining predicted sites, K44, K281, K355 and K363 were conserved in ~92% of the species while K51 is in 50% and K121 is found in ~17%. The preservation of predicted lysine residues between species suggests that FDH from Arabidopsis may not be unique in its regulation by the UPS

3.3. Arabidopsis FDH is Ubiquitinated *In Planta*

The above results, which demonstrate the turnover of FDH by the 26S proteasome and the presence of predicted ubiquitination sites, suggest that FDH is ubiquitinated in plant cells. FDH ubiquitination *in planta* was assessed by using ubiquitin-trap beads to isolate ubiquitinated proteins followed by western blot analysis to determine if FDH was among the isolated proteins. If CFP-HA-FDH is ubiquitinated *in planta* then the ubiquitin-trap beads should be able to isolate the enzyme from the protein extract. Total protein extract from tobacco tissue transiently expressing CFP-HA-FDH was incubated with ubiquitin-trap beads that utilized the ubiquitin-associated protein domain (UBA) to bind ubiquitinated proteins. Immunoblot analysis with antibodies that recognize the HA tag demonstrated that CFP-HA-FDH was among the pulled-down isolates, indicating that FDH is ubiquitinated *in planta* (Figure 3-4).

A

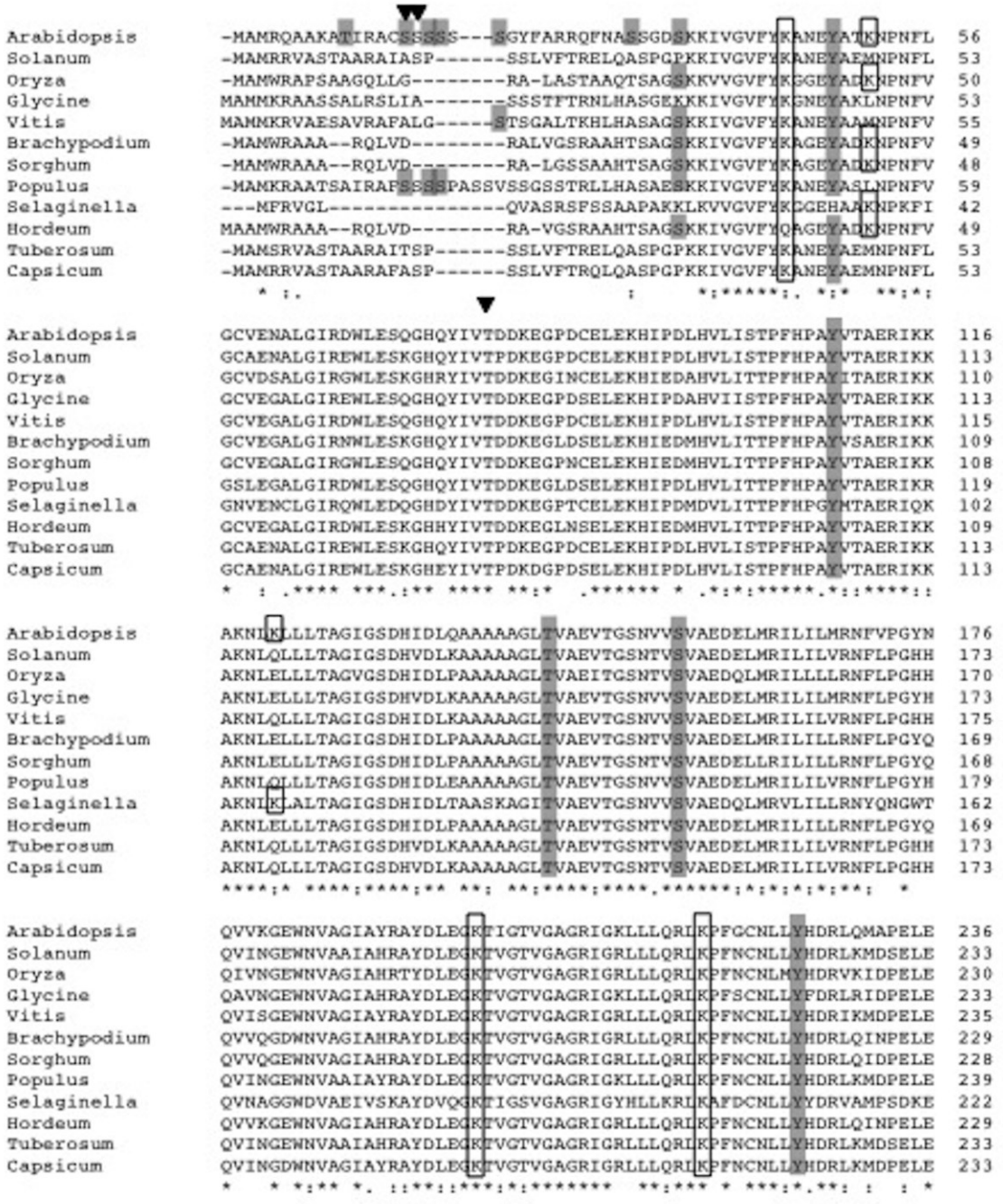
Arabidopsis
Solanum
Oryza
Glycine
Vitis
Brachypodium
Sorghum
Populus
Selaginella
Hordeum
Tuberosum
Capsicum

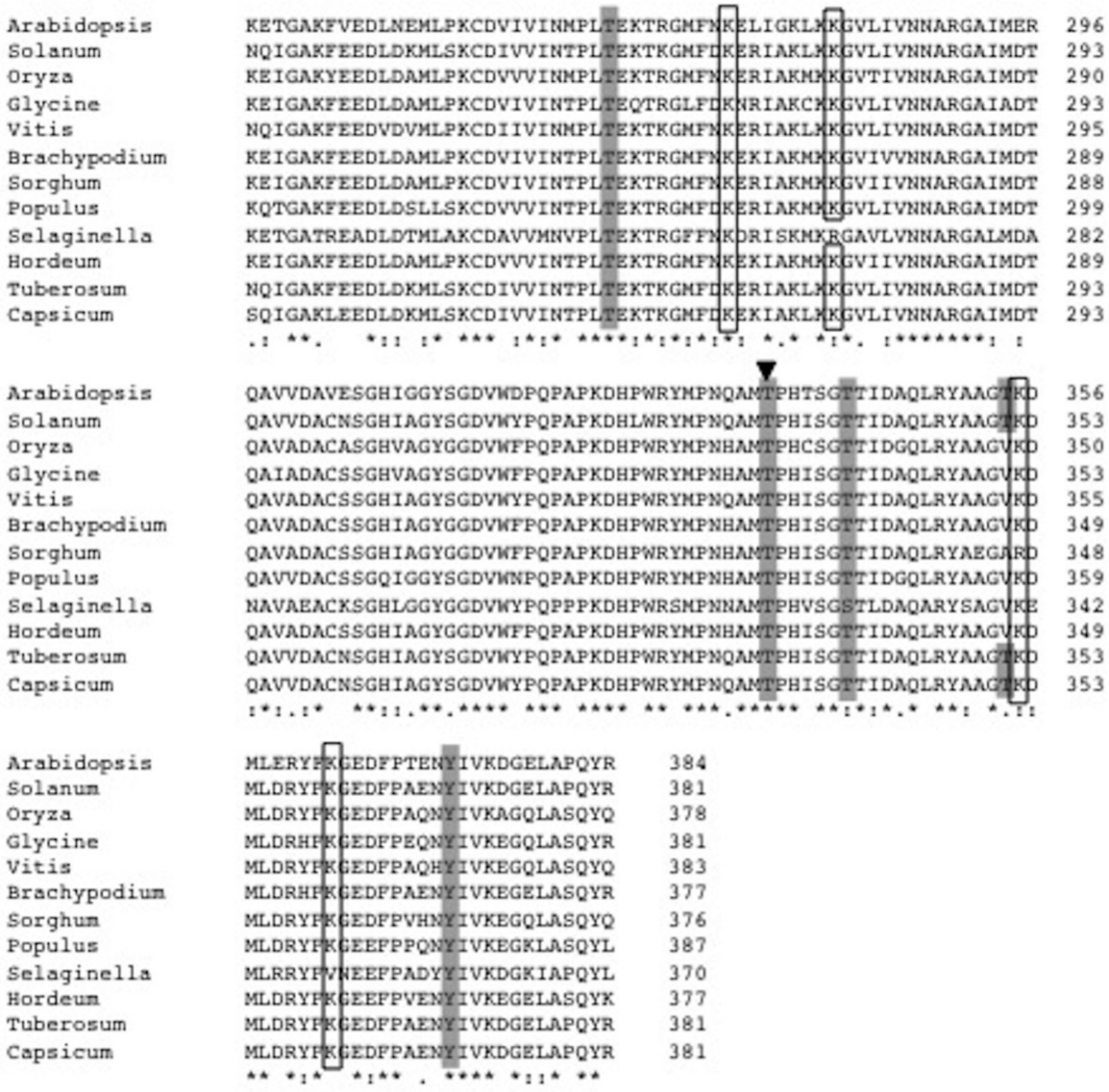
Arabidopsis KETGAKFVEDLNEMLPKCDVIVINMPLTEKTRGMFNKELIGKLKKGVLIVNNARGAIMER 296
Solanum NQIGAKFEEDLDKMLSKCDIVVINTPLTEKTKGMFDKERIAKLKKGVLIVNNARGAIMDT 293
Oryza KEIGAKYEEDLDAMLPKCDVVVINMPLTEKTRGMFNKERIAKMKKGVTIVNNARGAIMDT 290
Glycine KEIGAKFEEDLDAMLPKCDVIVINTPLTEQTRGLFDKNRIAKCKKGVLIVNNARGAIADT 293
Vitis NQIGAKFEEDVDVMLPKCDIIVINMPLTEKTKGMFNKERIAKLKKGVLIVNNARGAIMDT 295
Brachypodium KEIGAKFEEDLDAMLPKCDVIVINTPLTEKTRGMFNKEKIAKMKKGVIVVNNARGAIMDT 289
Sorghum KEIGAKFEEDLDAMLPKCDVIVINTPLTEKTRGMFNKERIAKMKKGVIIVNNARGAIMDT 288
Populus KQTGAKFEEDLDSLLSKCDVVVINTPLTEKTRGMFDKERIAKMKKGVLIVNNARGAIMDT 299
Selaginella KETGATREADLDTMLAKCDAVVMNVPLTEKTRGFFNKDRISKMKRGAVLVNNARGALMDA 282
Hordeum KEIGAKFEEDLDAMLPKCDVVVINTPLTEKTRGMFNKEKIAKMKKGVIIVNNARGAIMDT 289
Tuberosum NQIGAKFEEDLDKMLSKCDIVVINTPLTEKTKGMFDKERIAKLKKGVLIVNNARGAIMDT 293
Capsicum SQIGAKLEEDLDKMLSKCDIVVINTPLTEKTKGMFDKEKIAKLKKGVLIVNNARGAIMDT 293
QAVVDAVESGHIGGYSGDVWDPQPAPKDHPWRYMPNQAMTPHTSGTTIDAQLRYAAGTKD 356
QAVVDACNSGHIAGYSGDVWYPQPAPKDHLWRYMPNQAMTPHISGTTIDAQLRYAAGTKD 353
QAVADACASGHVAGYGGDVWFPQPAPKDHPWRYMPNHAMTPHCSGTTIDGQLRYAAGVKD 350
QAIADACSSGHVAGYSGDVWFPQPAPKDHPWRYMPNHAMTPHISGTTIDAQLRYAAGVKD 353
QAVADACSSGHIAGYSGDVWYPQPAPKDHPWRYMPNQAMTPHISGTTIDAQLRYAAGVKD 355
QAVADACSSGHIAGYGGDVWFPQPAPKDHPWRYMPNHAMTPHISGTTIDAQLRYAAGVKD 349
QAVADACSSGHIAGYGGDVWFPQPAPKDHPWRYMPNHAMTPHISGTTIDAQLRYAEGARD 348
QAVVDACSSGQIGGYSGDVWNPQPAPKDHPWRYMPNHAMTPHISGTTIDGQLRYAAGVKD 359
NAVAEACKSGHLGGYGGDVWYPQPPPKDHPWRSMPNNAMTPHVSGSTLDAQARYSAGVKE 342
QAVADACSSGHIAGYGGDVWFPQPAPKDHPWRYMPNHAMTPHISGTTIDAQLRYAAGVKD 349
QAVVDACNSGHIAGYSGDVWYPQPAPKDHPWRYMPNQAMTPHISGTTIDAQLRYAAGTKD 353
QAVVDACNSGHIAGYSGDVWYPQPAPKDHPWRYMPNQAMTPHISGTTIDAQLRYAAGTKD 353
MLERYPKGEDFPTENYIVKDGELAPQYR 384
MLDRYPKGEDFPAENYIVKDGELAPQYR 381
MLDRYPKGEDFPAQNYIVKAGQLASQYQ 378
MLDRHPKGEDFPEQNYIVKEGQLASQYR 381
MLDRYPKGEDFPAQHYIVKEGQLASQYQ 383
MLDRHPKGEDFPAENYIVKEGELASQYR 377
MLDRYPKGEDFPVHNYIVKEGQLASQYQ 376
MLDRYPKGEEFPPQNYIVKEGKLASQYL 387
MLRRYPVNEEFPADYYIVKDGKIAPQYL 370
MLDRYPKGEEFPVENYIVKEGELASQYK 377
MLDRYPKGEDFPAENYIVKDGELAPQYR 381
MLDRYPKGEDFPAENYIVKDGELAPQYR 381

B

	Arabidopsis thaliana	*Solanum lycopersicum*	*Oryza sativa*	*Glycine max*	*Vitis vinifera*	*Brachypodium distachyon*	*Sorghum bicolor*	*Populus trichocarpa*	*Selaginella moellendorffii*	*Hordeum vulgare*	*Solanum tubersum*	*Capsicum annuum*
Arabidopsis thaliana	100.00	81.36	75.93	78.95	81.41	80.64	80.85	80.99	66.22	80.59	81.36	81.10
Solanum lycopersicum	81.36	100.00	78.84	82.37	87.40	81.96	81.12	84.78	64.86	81.38	99.21	96.59
Oryza sativa	75.93	78.84	100.00	80.42	80.69	86.70	88.30	79.10	66.12	87.23	79.10	78.31
Glycine max	78.95	82.37	80.42	100.00	84.78	83.82	83.78	84.47	63.78	83.29	82.63	81.84
Vitis vinifera	81.41	87.40	80.69	84.78	100.00	83.02	84.57	86.39	66.22	83.29	87.40	86.88
Brachypodium distachyon	80.64	81.96	86.70	83.82	83.02	100.00	94.41	83.02	65.95	96.28	82.23	82.49
Sorghum bicolor	80.85	81.12	88.30	83.78	84.57	94.41	100.00	82.98	66.40	94.41	81.38	80.05
Populus trichocarpa	80.99	84.78	79.10	84.47	86.39	83.02	82.98	100.00	65.95	84.04	85.04	84.51
Selaginella moellendorffii	66.22	64.86	66.12	63.78	66.22	65.95	66.40	65.95	100.00	66.67	65.14	64.05
Hordeum vulgare	80.59	81.38	87.23	83.29	83.29	96.28	94.41	84.04	66.67	100.00	81.65	81.65
Solanum tubersum	81.36	99.21	79.10	82.63	87.40	82.23	81.38	85.04	65.14	81.65	100.00	96.33
Capsicum annuum	81.10	96.59	78.31	81.84	86.88	82.49	80.05	84.51	64.05	81.65	96.33	100.00

Figure 3-3: Sequence Alignment Matrix. A) Conservation of post-translational modifications. FDH protein sequences from 12 plant species aligned using Clustal Omega alignment program. Predicted ubiquitination sites (black outline), predicted phosphorylation sites (grey boxes) and experimentally observed phosphorylation sites (black arrowheads) are shown. Arabidopsis represents *Arabidopsis thaliana*, Solanum represents *Solanum lycopersicum*, Oryza represents *Oryza sativa Japonica*, Glycine represents *Glycine max*, Vitis represents *Vitis vinifera*, Brachypodium represents *Brachypodium distachyon*, Sorghum represents *Sorghum bicolor*, Populus represents *Populus trichocarpa*, Selaginella represents *Selaginella moellendorffii*, Hordeum represents *Hordeum vulgare*, Tuberosum represents *Solanum tuberosum* and Capsicum represents *Capsicum annuum.* Below the alignments, the asterisk (*) indicates a fully conserved residue, the colon (:) indicates that the amino acids have highly similar properties, the period (.) indicates that the amino acids have weakly similar properties B) The percentage similarity of FDH protein sequences from 12 plant species.

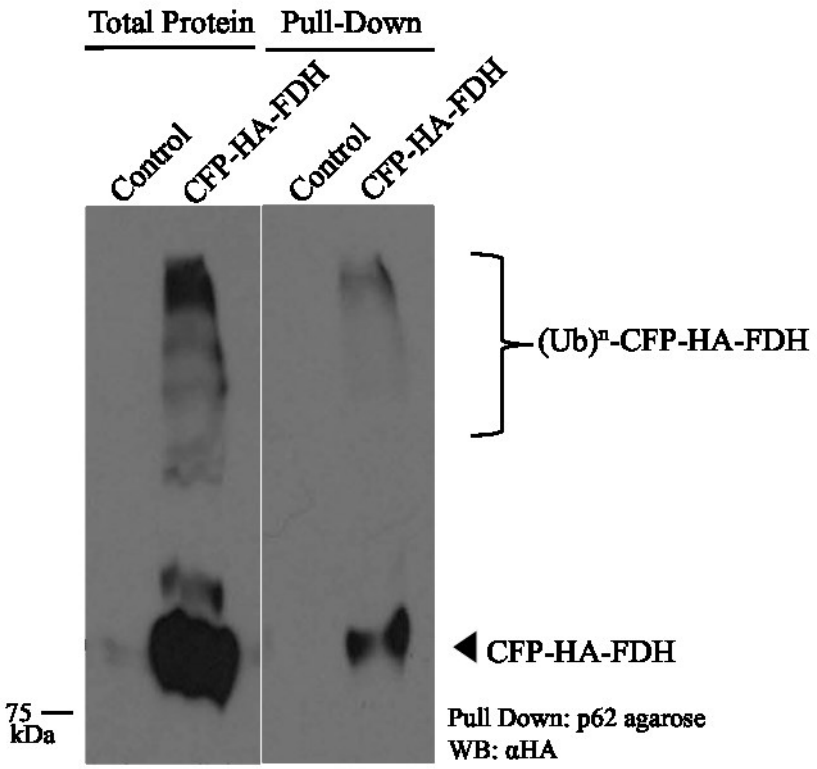

Figure 3-4: Ubiquitin Pull-Down Assay. Total protein extract was obtained from infiltrated tobacco tissue transiently expressing CFP-HA-FDH or from uninfiltrated tobacco tissue (control). Extracts were incubated with ubiquitin-trap beads (p62 agarose) to isolate ubiquitinated proteins. Proteins were eluted from the beads and subjected to SDS-PAGE and western blot (WB) probing for the HA tag fused to CFP-HA-FDH. Note the presence of CFP-HA-FDH in the pulled down sample.

3.4. KEG is Involved in FDH Turnover

Previous results implicating KEG as an FDH interacting protein suggests that the E3 ligase targets FDH for degradation (Schofield, unpublished). To investigate this possibility, an *in vitro* ubiquitination assay was used to determine if KEG attaches ubiquitin molecules to FDH. Following the ubiquitination assay, higher migrating forms of FDH were observed by western blot analysis, demonstrating that KEG attaches ubiquitin to FDH. The higher migrating forms of FDH were not observed in assays where ubiquitin was omitted from the reaction (Figure 3-5).

The next aim was to determine if KEG is involved in FDH turnover in plant cells. Transiently transformed tobacco tissue expressing CFP-HA-FDH or co-expressing CFP-HA-FDH and HA-KEG were used in cell free degradation assays. If KEG is involved in FDH degradation then co-expression of FDH with KEG should result in an increase in FDH degradation. When CFP-HA-FDH was co-expressed with HA-KEG the amount of CFP-HA-FDH decreased much faster than when CFP-HA-FDH was expressed by itself (Figure 3-6A and 3-6B and Supplementary Figure S2). Pixel intensity analysis revealed the difference in CFP-HA-FDH abundance over time (Figure 3-6C). The faster rate of FDH turnover in the presence of KEG suggests that the E3 ligase is involved in targeting the enzyme to the 26S proteasome for degradation.

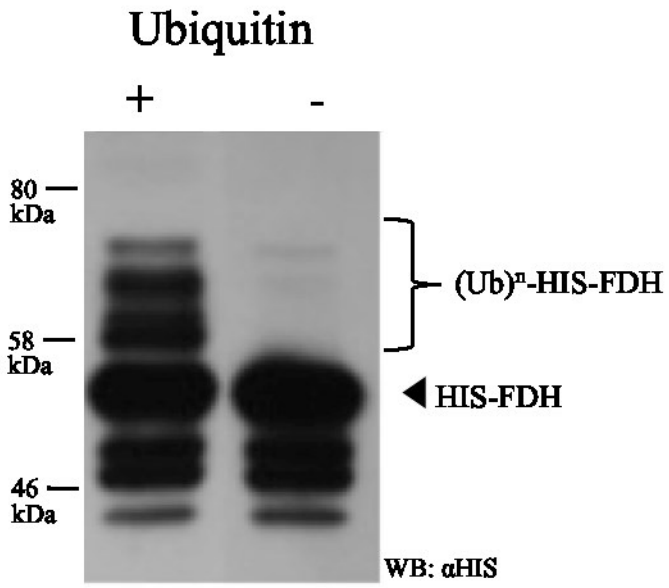

Figure 3-5: Ubiquitination Assay. Purified HIS-FDH was mixed with ubiquitin-activating enzyme (E1), ubiquitin conjugating enzyme (E2) and the E3 ubiquitin ligase KEG in the presence or absence of ubiquitin molecules. Note the higher migrating forms of HIS-FDH in the reaction that was supplemented with ubiquitin, representing the ubiquitinated protein ($(Ub)^n$-HIS-FDH) (Schofield, unpublished).

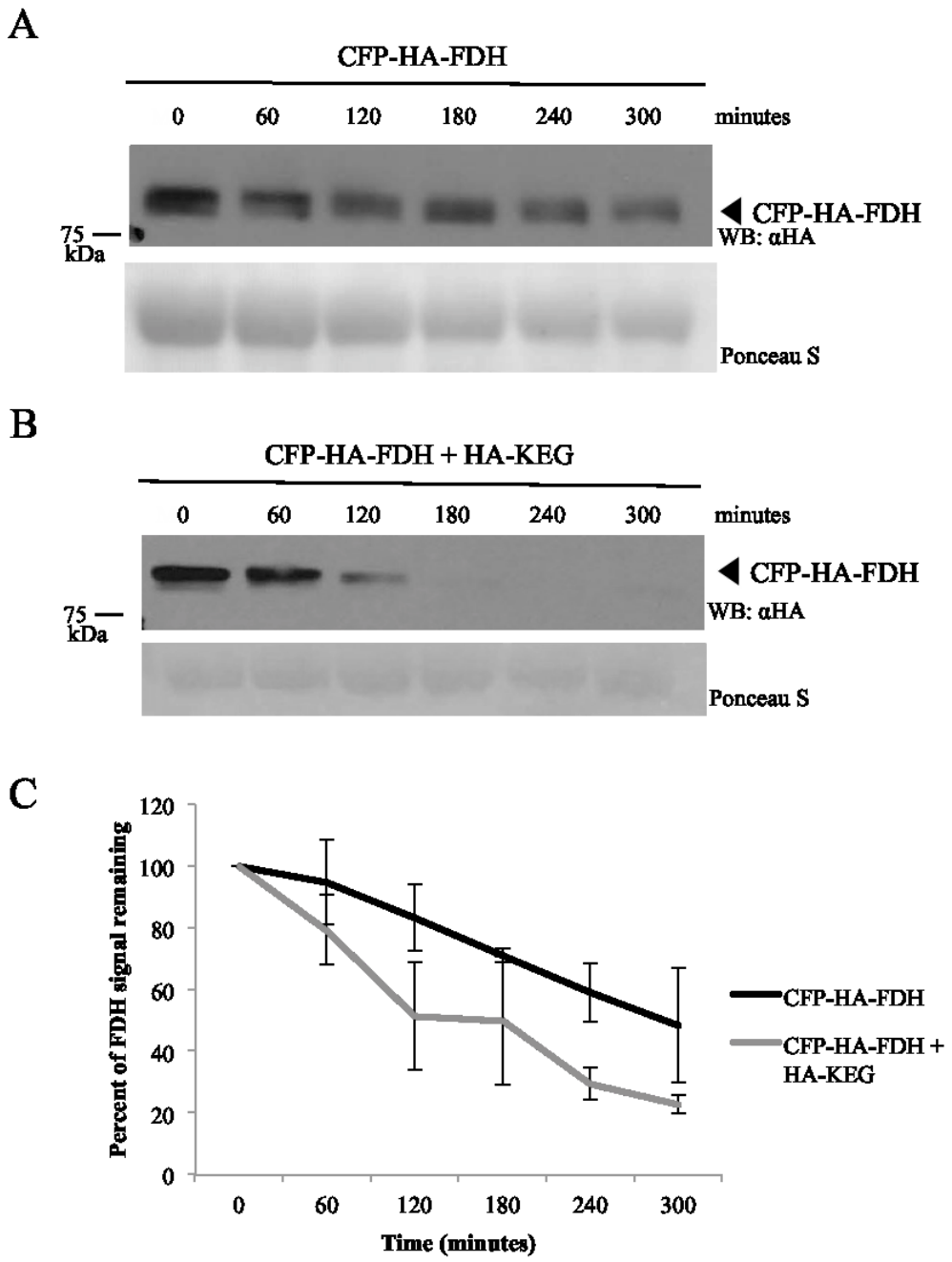

Figure 3-6: FDH Degradation Is Dependent On KEG. Representative cell free degradation assay using tobacco tissue A) transiently expressing CFP-HA-FDH and B) tobacco tissue transiently co-expressing CFP-HA-FDH with HA-KEG. Total protein was extracted from each of the tissues and the abundance of FDH was observed over time. Protein samples were subjected to SDS-PAGE and immunoblot analysis with antibodies that recognize HA. C) Average pixel intensity of CFP-HA-FDH protein bands from the representative and replicated cell free degradation assays showing the percent of FDH remaining over time. Bars represent the standard error of mean (n=2). Ponceau S shows the protein loading in each lane.

3.5. A Functional KEG E3 Ligase is Required for FDH Turnover

The above results clearly demonstrate a role for KEG in FDH degradation. However, it was important to clarify that the disappearance of FDH observed in previous cell free degradation assays was directly due to KEG activity and not another E3 ligase in the protein extract. To accomplish this, transiently transformed tobacco tissue co-expressing CFP-HA-FDH with either HA-KEG or HA-KEG^{AA}, the latter with a non-functional RING domain, were used in cell free degradation assays. If KEG is responsible for ubiquitinating FDH, then a functional RING domain would be essential to the proteolysis of the enzyme. When CFP-HA-FDH was co-expressed with HA-KEG^{AA} its degradation rate was slower than when it was co-expressed with HA-KEG (Figure 3-7A and 3-7B and Supplementary Figure S-3). Pixel intensity analysis revealed the difference in CFP-HA-FDH abundance over time (Figure 3-7C). Slower degradation in the presence of a RING-mutated KEG implies that the turnover of FDH is dependent on the RING domain of the E3 ligase.

3.6. Arabidopsis FDH is Phosphorylated *In Planta*

Evidence of phosphorylation on FDH from *Solanum tuberosum* (potato) prompted a search for phosphorylation sites on FDH from Arabidopsis. Through the use of phosphorylation site prediction software the extent to which Arabidopsis FDH could be phosphorylated was established. Seven serine, six threonine and four tyrosine residues were identified as hypothetical phosphorylation sites (Figure 3-2 and Supplementary Table S-8). These results indicate that FDH from Arabidopsis has the potential to be phosphorylated, similar to the phosphorylation of FDH in potato.

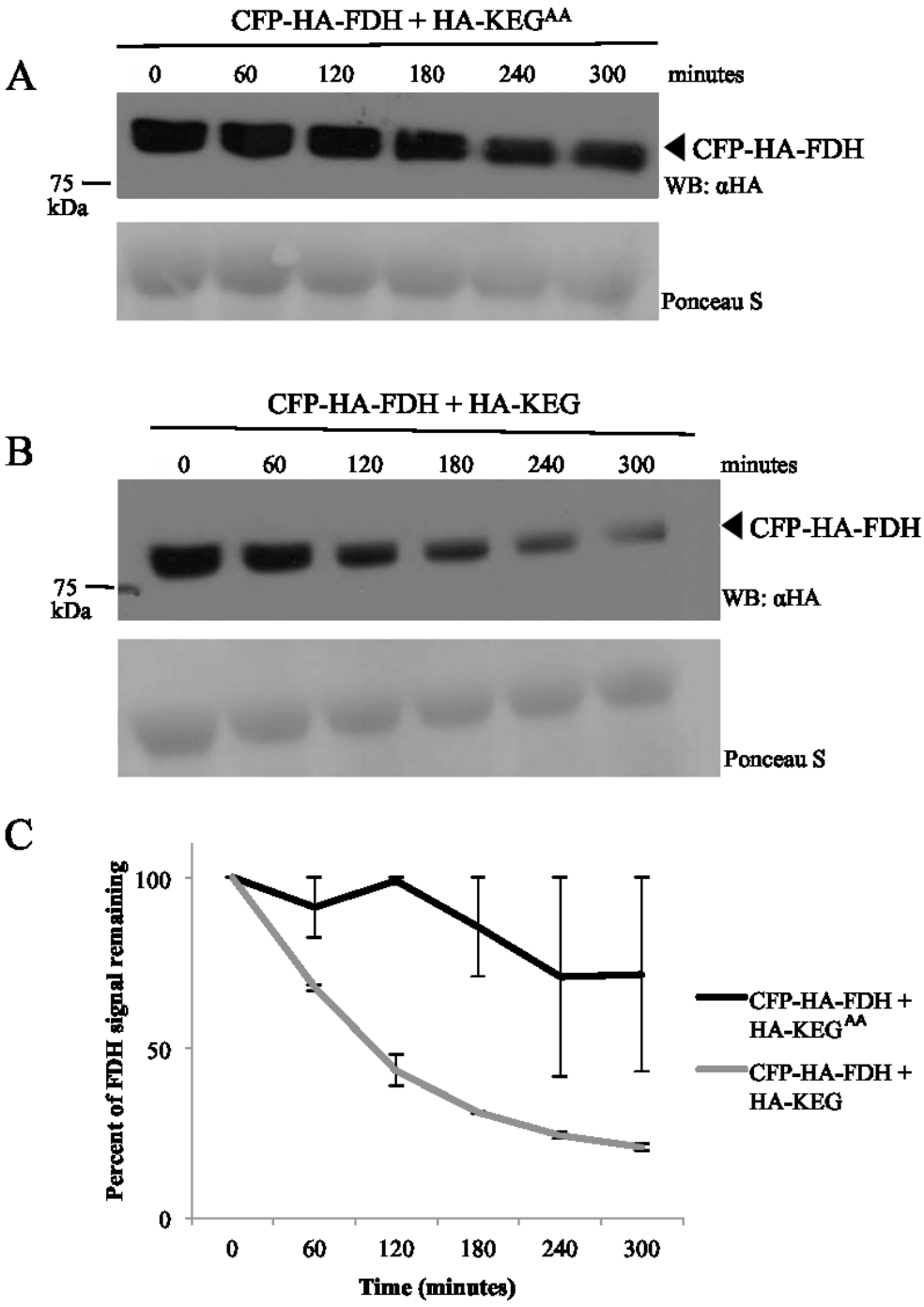
A
CFP-HA-FDH + HA-KEG^AA
0
60
120
180
240
300
minutes
CFP-HA-FDH
75 kDa
WB: αHA
Ponceau S
B
CFP-HA-FDH + HA-KEG
0
60
120
180
240
300
minutes
CFP-HA-FDH
75 kDa
WB: αHA
Ponceau S
C
Percent of FDH signal remaining
100
50
0
0
60
120
180
240
300
Time (minutes)
CFP-HA-FDH + HA-KEG^AA
CFP-HA-FDH + HA-KEG

Figure 3-7: FDH Degradation Requires A Functional RING Domain. Representative cell free degradation assay using tobacco tissue A) transiently co-expressing CFP-HA-FDH with HA+ KEG^{AA} and B) tobacco tissue transiently co-expressing CFP-HA-FDH with HA-KEG. KEG^{AA} was rendered non-functional by mutating the RING domain so KEG could no longer ubiquitinate proteins. Total protein was extracted from each of the tissues and the abundance of FDH was observed over time by removing equal volumes of sample from each of the protein extracts at the indicated time points. Protein samples were subjected to SDS-PAGE and immunoblot analysis with antibodies that recognize HA. C) Average pixel intensity of CFP-HA-FDH protein bands from the representative and replicated cell free degradation assays showing the percent of FDH remaining over time. Bars represent the standard error of mean (n=2). Ponceau S shows the protein loading in each lane.

To determine if the phosphorylation potential of FDH from Arabidopsis is shared between other organisms, a protein sequence alignment of FDH from 11 other plant species was conducted. It was determined that nine of the 17 predicted phosphorylation sites identified in Arabidopsis FDH were conserved in all of the other sequences (Figure 3-3A). The conservation of predicted phosphorylation sites between plant FDHs suggests that the modification of this enzyme by phosphorylation may not be unique to Arabidopsis. FDH from Arabidopsis shares at least 80% amino acid sequence similarity with FDH from the other plant species aligned, except for *Glycine max* (soybean), *Oryza sativa* (rice) and *Selaginella moellendorffii*, the latter being an ancient vascular species (Figure 3-3B).

To confirm that Arabidopsis FDH is phosphorylated *in vivo,* protein extract from tobacco tissue transiently expressing CFP-HA-FDH was immunoprecipitated and probed with an anti-phosphoserine antibody. If CFP-HA-FDH is phosphorylated, then incubation with an antibody specific to serine phosphorylation should bind to CFP-HA-FDH allowing it to be visualized by western blotting. The results of that western blot demonstrate that CFP-HA-FDH is phosphorylated *in vivo* (Figure 3-8 and Supplemental Figure S-6).

To provide further evidence for FDH phosphorylation, protein extracts from tobacco tissue transiently expressing *CFP-HA-FDH* were incubated with an alkaline phosphatase followed by western blot analysis with HA antibodies. Dephosphorylation of FDH is evident in the shift in the migration of CFP-HA-FDH (Figure 3-9A). An interesting observation is that samples containing CFP-HA-FDH that were treated with the alkaline phosphatase appeared to be more stable than un-treated samples, as indicated by the band's darker appearance (Figure 3-9A and Supplementary Figure S-4). Pixel intensity analysis was used to determine the difference in CFP-HA-FDH abundance (Figure 3-9B). This result suggests that the

dephosphorylated form of FDH is more stable and that phosphorylation may contribute to the degradation of the enzyme.

3.7. KEG Overexpressing Plants are More Tolerant of Formate Stress

Since KEG appears to be regulating FDH, an enzyme that removes formate from the cell, it was important to determine if KEG is involved in regulating plant responses to formate stress. A formate sensitivity assay was conducted to compare the root growth of wild type (WT) and transgenic seedlings constitutively overexpressing *KEG* (*KEG O/E*) grown in the presence and absence of formate. If KEG is targeting FDH for degradation, then plants constitutively overexpressing the E3 ligase should have less of the enzyme present than WT plants, which suggests that *KEG O/E* would be less efficient at removing formate from their system. Excess formate has been shown to be toxic to plant systems and impede growth. Therefore, the *KEG O/E* lines should be more sensitive to the presence of formate, which should be reflected by the greater inhibition of root growth compared to WT. At 48 hours, the average root length of WT plants was similar whether they were grown in the presence or absence of formate with only 4% inhibition observed (Figure 3-10A, 3-10B and Supplementary Figure S-5). However, the average root length of KEG O/E plants was significantly shorter when they were grown in the presence of formate with a 27% inhibition observed. At 72 hours, both WT and KEG O/E roots were shorter than when grown in the presence of formate (Figure 3-10), however *KEG O/E* lines were inhibited more severely with 31% root growth inhibition (Figure 3-10B). The higher sensitivity of *KEG O/E* to the presence of formate is an indication that KEG is negatively affecting plant response to formate.

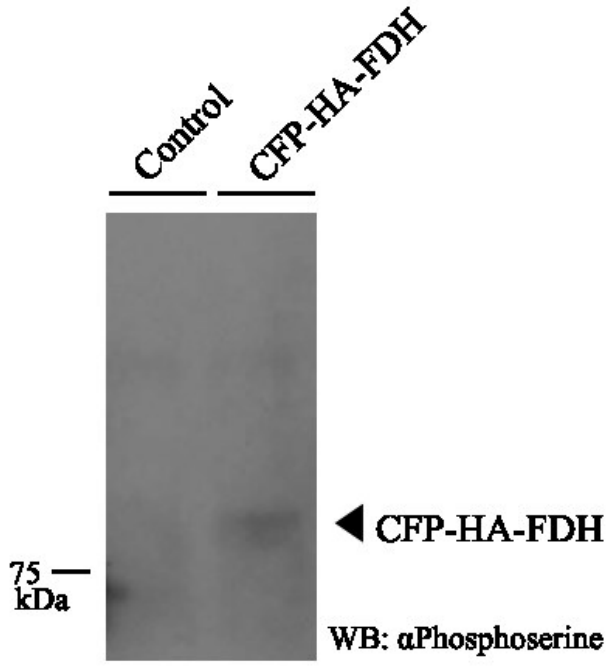

Figure 3-8: FDH is Phosphorylated *In Planta*. Total protein was extracted from infiltrated tobacco tissue transiently expressing CFP-HA-FDH and un-infiltrated tobacco tissue (control). The resulting extracts were immunoprecipitated and subjected to immunoblot analysis with a phosphoserine specific antibody that identified CFP-HA-FDH as a phosphorylated protein.

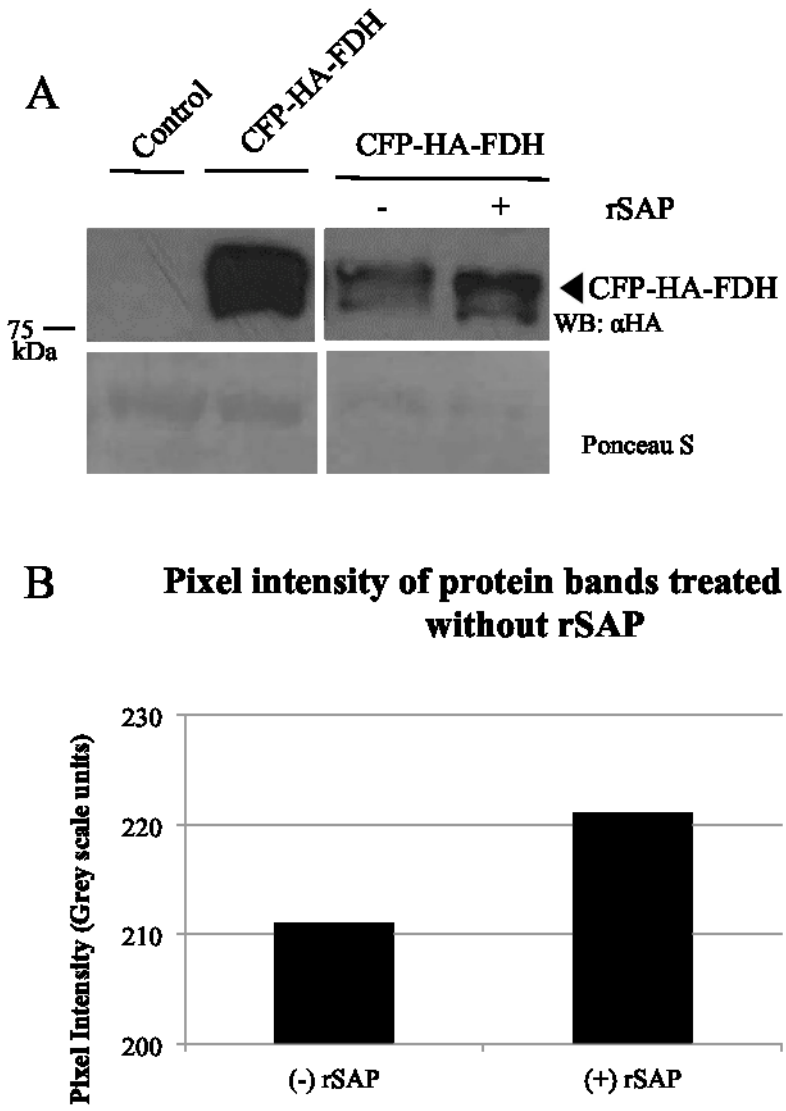

Figure 3-9: Dephosphorylation Assay. A) Total protein extract containing CFP-HA-FDH was equally divided into two treatments that were either incubated with (+) or without (-) an alkaline phosphatase (rSAP). Protein samples were then subjected to SDS-PAGE and immunoblot analysis with antibodies that recognize HA. Un-infiltrated tissue served as the control. Note that rSAP treated FDH has a lower molecular weight and a darker band. Ponceau S shows protein loading. B) Graph shows pixel intensity of FDH following treatment with (+) or without (+) rSAP.

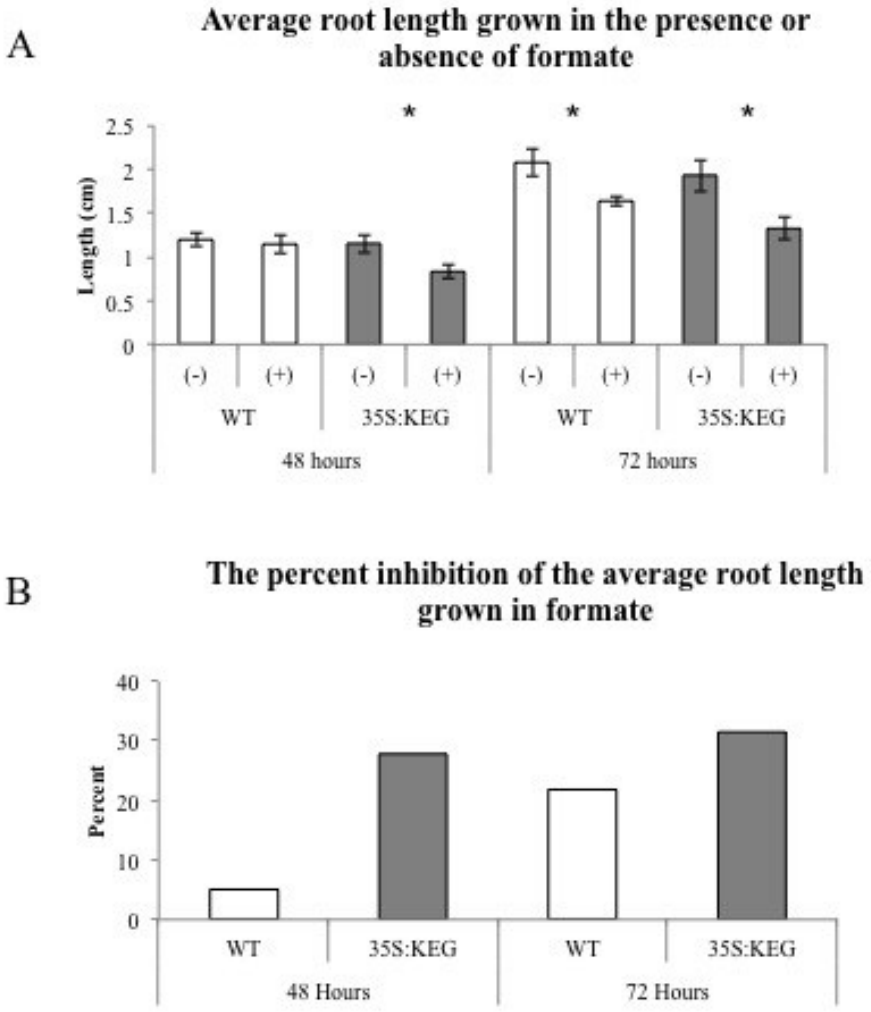

Figure 3-10: Formate Sensitivity Analysis. A) Average root length grown in the presence (+) or absence (-) of formate. Bars represent the mean primary root length of each genotype +/- standard error of the sample (n= 12). Wild type (WT) and transgenic Arabidopsis plants constitutively expressing KEG (35S:KEG) were grown on standard ½ Murashige and Skoog (MS) media +/- formate. Asterisks indicate a statistically significant ($p < 0.05$) difference between mean root lengths within genotypes. B) The percent inhibition of the average root length grown in the presence of formate. In both 48 and 72 hours times point's 35S:KEG is inhibited to a higher degree than WT.

CHAPTER FOUR: DISCUSSION

4.1. Ubiquitination of FDH

Previously, a high throughput yeast-two hybrid screen suggested that the RING-type E3 ligase KEG interacts with the stress response protein FDH (Schofield, unpublished). Further investigation using a GST pull-down technique confirmed the interaction and demonstrated that the connection required the HERC-like repeats of KEG (Schofield, unpublished). The purpose of this study was to investigate the functional significance of the interaction between KEG and FDH in plant systems. As demonstrated by using cell free degradation assays, FDH is turned over by the 26S proteasome and KEG in involved in targeting FDH for degradation. This provides strong evidence for a functional relationship between KEG and FDH in plant cells as regulator and substrate, respectively. Through the use of prediction software, *in vitro* ubiquitin assays and an *in planta* ubiquitin pull down assay, this study has provided convincing evidence that FDH is ubiquitinated. Since FDH is degraded in a 26S proteasome-dependant manner, it is expected that FDH is modified by ubiquitin addition, signalling for enzyme's interaction with the proteasome. In a literature search of high-throughput mass spectrometry studies, focusing on the Arabidopsis ubiquitome, it was found that another study identified FDH as a ubiquitinated protein (Kim et al., 2013). The mass spectrometry data on the ubiquitination state of FDH supports the argument made in this study that the abundance and function of FDH in Arabidopsis is regulated by the UPS.

4.2. KEG Facilitates the Degradation of FDH

Due to the interaction of KEG with FDH and the evidence pointing to the 26S proteasome-dependant degradation of the enzyme it was hypothesized that KEG plays a role in regulating FDH abundance. The results presented provide strong evidence that KEG, specifically its

RING domain, modulates FDH protein abundance. This is the first time that regulation of FDH function by the UPS has been demonstrated. Due to the unique domain architecture of KEG (Figure 1-4), containing a kinase domain, investigation into the kinase activity of KEG and how it affects FDH degradation merits more detailed exploration. Observing the stability of FDH in the presence of either a kinase dead form of KEG or a version of KEG that has a constitutively active kinase domain is of future interest to this study.

4.3. FDH Degradation and Formate Sensitivity

It is established that formate has a toxic effect on plant systems (David et al., 2010) and that FDH's biochemical role is to convert formate into CO_2 (Popov and Lamzin, 1994), effectively removing formate, and limiting its toxic effect on the cell and the plant. Li et al., 2002 concluded that Arabidopsis seedlings overexpressing *FDH* on a constitutive promoter were less sensitive to the exogenous addition of formate into their growth medium than WT Arabidopsis under the same conditions, as indicated by unhindered root growth. These plants are more efficient than WT at removing formate from their cells because they have a higher abundance of FDH. Replication of this experiment using WT and transgenic Arabidopsis seedlings constitutively overexpressing *KEG* showed that the transgenic seedlings were more sensitive to the presence of exogenous formate than WT Arabidopsis seedlings were under the same conditions (Figure 3-11). In combination with the Li et al., 2002 investigation, the increased sensitivity of *KEG* overexpressing seedlings suggests that these plants are unable to remove the excess formate as efficiently as WT and as a result they experience a greater toxic effect. One explanation for this could be that the increased expression of *KEG* leads to a more efficient removal of FDH via the UPS. With less FDH available, formate remains in the cells longer, imposing toxic effects on root growth.

4.4. Cross Talk between Phosphorylation and Ubiquitination

Cross talk between different post-translational modifications has become more apparent in recent years due to the increased availability of mass spectrometric data (Hunter, 2007). Research in this area has identified putative trends such as the synergistic and antagonistic effects of phosphorylation on ubiquitination. For example, the protein kinase complex, IκB, is involved in the cellular inflammation response. The degradation of IκB is a result of the E3 ligase, β-transducin repeat containing protein (β-TRCP), recognizing it as a substrate for ubiquitination. The identification of IκB as a substrate for degradation by β-TRCP is triggered by the phosphorylation of IκB (Lecker, 2006). In another example the phosphorylation of the E3 ligase, neural precursor cell expressed developmentally down-regulated protein (NEDD) 4, inhibits its ability to target the amiloride-sensitive sodium channel (ENaC) for degradation (Ichimura et al., 2005). FDH possesses multiple experimentally identified and theoretical phosphorylation sites (Blom et al., 1999; Bykova et al., 2003; Roitinger et al., 2015; Xue et al., 2013) that could regulate modifications such as ubiquitination.

Results from this study as well as work from previous publications suggest that Arabidopsis FDH is phosphorylated (Blom et al., 1999; Bykova et al., 2003; Roitinger et al., 2015; Xue et al., 2013). Of particular interest to this study is the differential phosphorylation observed on S16 in Arabidopsis FDH when subjected to stress-inducing conditions (Xue et al., 2013). Under normal conditions both S15 and S16 are phosphorylated, but when treated with ABA or mannitol, S16 was not identified as a phosphorylated residue (Roitinger et al., 2015; Xue et al., 2013). The difference in phosphorylation suggests that S16 is a stress-regulated phosphorylation or de-phosphorylation site since ABA is a stress hormone and mannitol induces osmotic stress in plants. This may explain why Arabidopsis FDH appears more stable

when it is treated with an alkaline phosphatase (Figure 3-8). If the phosphorylation of S16 on FDH is required for KEG to recognize FDH as a substrate for ubiquitination, then the complete dephosphorylation of FDH by the phosphatase would render FDH unidentifiable by KEG, contributing to the stability of the enzyme.

4.5. Model for KEG Regulation of FDH Function

The origin of formate in plant tissues remains unclear. There are various cellular pathways that may produce formate as a by-product but experimental evidence to support these theories is lacking (Hourton-Cabassa et al., 1998; Igamberdiev et al., 1999). What is clear is that higher plants do have small metabolically active pools of formate (Hanson and Roje, 2001). Under stressful conditions, such as drought, the amount of formate increases and this correlates with the amplified expression of *FDH* (Ambard-Bretteville et al., 2003). Previous studies have identified FDH as a stress response protein and have investigated the downstream effects that FDH has on promoting stress responses (Choi et al., 2014). Until now, there has been a gap in our understanding of what lies upstream, regulating FDH on a molecular level. Experimental results from this study as well as prediction software and mass spectrometry data show that FDH is ubiquitinated and potentially differentially phosphorylated. The regulatory effects of these post-translational modifications on FDH, require further experimental investigation. Specifically, more evidence is needed to determine the importance of the phosphorylation state of S16 in regards to the stability of FDH.

With the data currently available it is hypothesized that the UPS regulates FDH abundance through its interaction with KEG. The model proposed is a variation of the model proposed by Choi et al., 2014 where it is suggested that FDH promotes the up regulation of SA and defence genes in response to pathogen attack. Evidence from this study showing that FDH is regulated

by KEG and how differential phosphorylation could play a role in the modulating enzyme stability has added to this model (Figure 4-1). The evidence suggests that under normal conditions FDH exists in a heavily phosphorylated form with both S15 and S16 phosphorylated (Roitinger et al., 2015). The heavily phosphorylated form of FDH may be recognized by the UPS, targeted for ubiquitination by KEG and degraded by the 26S proteasome, keeping FDH levels low in normal growth conditions (Figure 4-1A). When a stress is present, FDH levels rise and promote the expression of stress response proteins (Choi et al., 2014). Under the same conditions, ABA levels rise and promote the degradation of KEG (Liu and Stone, 2010). The increase in FDH abundance under stressful conditions could be due to the ABA-dependent degradation of KEG, the inability of KEG to identify FDH as a target for ubiquitination, or a combination of the two (Figure 4-1B). Following treatment with the stress simulating compounds, ABA and mannitol, FDH exists in a lightly phosphorylated form with only S15 phosphorylated (Xue et al., 2013). Dephosphorylation results from this study show that the dephosphorylated form of FDH was considerably more stable than the phosphorylated form. The change in FDH phosphorylation status may prohibit KEG from recognizing FDH as a substrate. Regardless, it is proposed that the change in phosphorylation, whether it is the de-phosphorylation of S16 or the inhibition of the kinase responsible for phosphorylating S16, protects FDH from degradation by the UPS when the plant is experiencing stress (Figure 4-1C).

Serine15 and S16 phosphorylation sites are not well conserved between the 12 species compared in Figure 3-3 although other phosphorylation sites are predicted to exist in these other species. Perhaps S16 proposed differential phosphorylation is specific to Arabidopsis FDH and other species have different residues that affect FDH stability.

The differential phosphorylation sites of FDH are found within the predicted mitochondrial-targeting signal (Figure 3-2). Typically these transit signals are removed after the protein is imported to their final destination. Due to the different localization patterns of KEG and FDH it is believed that these proteins interact before FDH is imported into the mitochondria. In that case, FDH would still possess the signalling peptide with the differential phosphorylation sites. Localization studies focusing on where KEG and FDH interact within the cell is an important next step to determine if this is a feasible scenario.

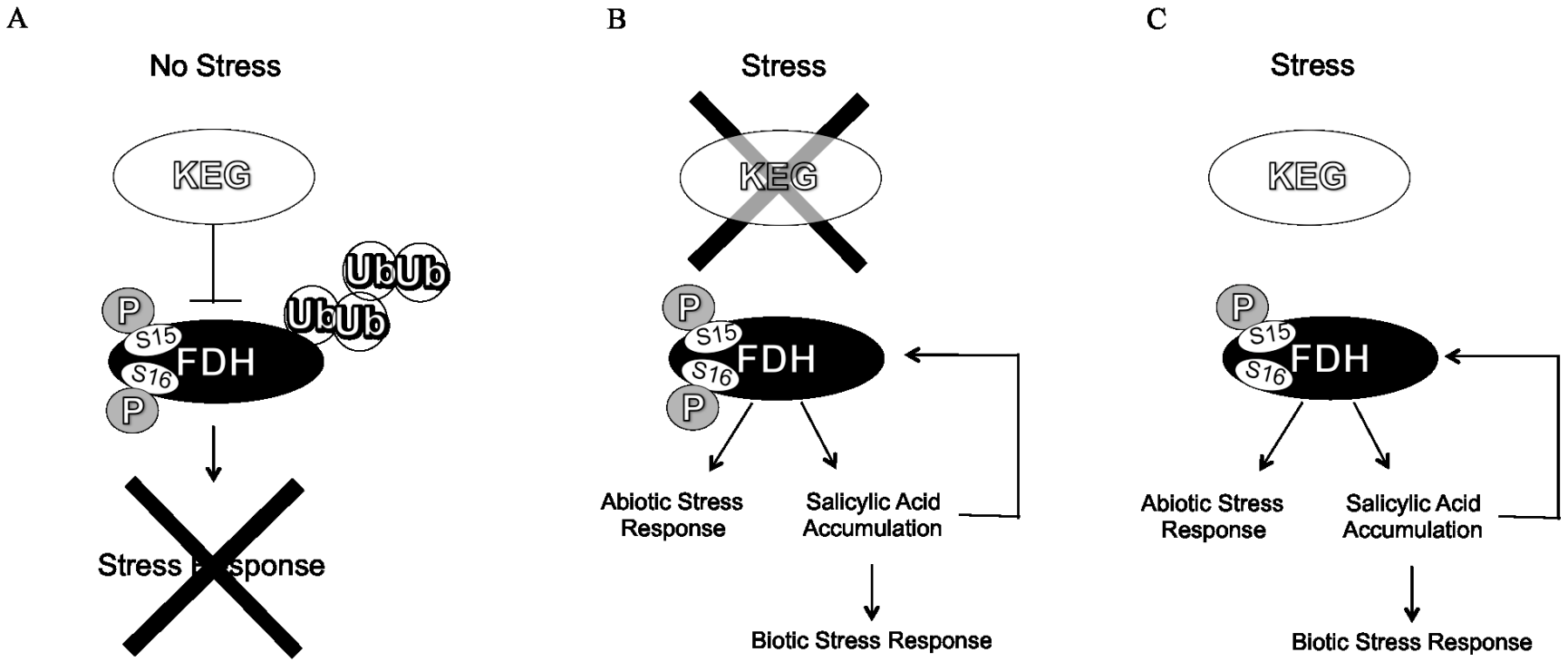

Figure 4-1: Model For The Regulation Of FDH By KEG. A schematic model representing the hypothetical interaction and process between FDH and KEG in the presence and absence of stress. A) In the absence of stress, FDH is phophorylated at Serine (S) 15 & S16. KEG recognizes the heavily phosphorylated form of FDH as a substrate for ubiquitination. The attachment of ubiquitin molecules sends FDH to the 26S proteasome and is degraded. As a result, no stress response is initiated. When stress is present, B) KEG interaction with FDH is inhibited by its ABA-dependent degradation or C) Serine 16 on FDH is dephosphorylated, rendering FDH unrecognizable by KEG. Potentially there is a combination of B and C. In any case, under stressful conditions FDH isn't identified as a target for ubiquitination which allows it to accumulate and signal for a down stream stress response which could be abiotic and biotic specific responses. For biotic stress response salicylic acid synthesis increases, which feeds back to promote the expression of FDH as well as other stress proteins, ultimately leading to a coping response to the perceived stress.

4.6. Summary

Under normal conditions KEG targets FDH for degradation via the UPS, keeping the enzyme level low to avoid an unnecessary stress response. This allows for small pools of cellular formate to exist, contributing to the synthesis of amino acids. Under stressful conditions, formate levels rise which is toxic to the cell. At the same time, FDH accumulates because KEG is unable to target the enzyme for degradation. The accumulation of FDH promotes stress responses such as the synthesis of SA, which promotes the expression of stress response genes. Ultimately, the appropriate coping response to the perceived stress is generated.

REFERENCES

Abràmofff, M. D., Magalhães, P. J., and Ram, S. J. (2005). Image processing with ImageJ Part II. *Biophotonics Int.* 11, 36–43. doi:10.1117/1.3589100.

Ambard-Bretteville, F., Sorin, C., Rébeillé, F., Hourton-Cabassa, C., and Colas des Francs-Small, C. (2003). Repression of formate dehydrogenase in Solanum tuberosum increases steady-state levels of formate and accelerates the accumulation of proline in response to osmotic stress. *Plant Mol. Biol.* 52, 1153–1168.

Besson, A., Gurian-West, M., Chen, X., Kelly-Spratt, K. S., Kemp, C. J., and Roberts, J. M. (2006). A pathway in quiescent cells that controls p27Kip1 stability, subcellular localization, and tumor suppression. *Genes Dev.* 20, 47–64. doi:10.1101/gad.1384406.

Blom, N., Gammeltoft, S., and Brunak, S. (1999). Sequence and structure-based prediction of eukaryotic protein phosphorylation sites. *J. Mol. Biol.* 294, 1351–62. doi:10.1006/jmbi.1999.3310.

Borden, K. L. (2000). RING domains: master builders of molecular scaffolds? *J. Mol. Biol.* 295, 1103–12. doi:10.1006/jmbi.1999.3429.

Brocard, I., Lynch, T., and Finkelstein, R. (2002). Regulation and role of the Arabidopsis abscisic acid-insensitive 5 gene in abscisic acid, sugar, and stress response. *Plant Physiol.* 129, 1533–1543. doi:10.1104/pp.005793.1.

Bykova, N. V., Stensballe, A., Egsgaard, H., Jensen, O. N., and Møller, I. M. (2003). Phosphorylation of formate dehydrogenase in potato tuber mitochondria. *J. Biol. Chem.* 278, 26021–26030. doi:10.1074/jbc.M300245200.

Callis, J., Carpenter, T., Sun, C. W., and Vierstra, R. D. (1995). Structure and evolution of genes encoding polyubiquitin and ubiquitin-like proteins in Arabidopsis thaliana ecotype Columbia. *Genetics* 139, 921–939.

Callis, J., and Vierstra, R. D. (2000). Protein degradation in signaling. *Curr. Opin. Plant Biol.* 3, 381–386. doi:10.1016/S1369-5266(00)00100-X.

Chen, X., Qiu, J. D., Shi, S. P., Suo, S. B., Huang, S. Y., and Liang, R. P. (2013a). Incorporating key position and amino acid residue features to identify general and species-specific Ubiquitin conjugation sites. *Bioinformatics* 29, 1614–1622. doi:10.1093/bioinformatics/btt196.

Chen, Y.-T., Liu, H., Stone, S., and Callis, J. (2013b). ABA and the ubiquitin E3 ligase KEEP ON GOING affect proteolysis of the Arabidopsis thaliana transcription factors ABF1 and ABF3. *Plant J.* 75, 965–76. doi:10.1111/tpj.12259.

Choi, D. S., Kim, N. H., and Hwang, B. K. (2014). Pepper Mitochondrial Formate Dehydrogenase1 Regulates Cell Death and Defense Responses against Bacterial Pathogens. *Plant Physiol.* 166, 1298–311. doi:10.1104/pp.114.246736.

Ciehanover, A., Hod, Y., and Hershko, A. (1978). A heat-stable polypeptide component of an ATP-dependent proteolytic system from reticulocytes. *Biochem. Biophys. Res. Commun.* 81, 1100–1105. doi:10.1016/0006-291X(78)91249-4.

Colas des Francs-Small, C., Ambard-Bretteville, F., Small, I. D., and Rémy, R. (1993). Identification of a major soluble protein in mitochondria from nonphotosynthetic tissues as NAD-dependent formate dehydrogenase. *Plant Physiol.* 102, 1171–1177. doi:10.1104/pp.102.4.1171.

David, P., des Francs-Small, C. C., Sévignac, M., Thareau, V., Macadré, C., Langin, T., et al. (2010). Three highly similar formate dehydrogenase genes located in the vicinity of the B4 resistance gene cluster are differentially expressed under biotic and abiotic stresses in Phaseolus vulgaris. *Theor. Appl. Genet.* 121, 87–103. doi:10.1007/s00122-010-1293-x.

Deshaies, R. J., and Joazeiro, C. a P. (2009). RING domain E3 ubiquitin ligases. *Annu. Rev. Biochem.* 78, 399–434. doi:10.1146/annurev.biochem.78.101807.093809.

Freemont, P. S. (1993). The RING Finger: A Novel Protein Sequence Motif Related to the Zinc Finger. *Ann. New York Acad. Sci.* 684, 174–192.

Glickman, M. H., and Ciechanover, A. (2002). The Ubiquitin-Proteasome Proteolytic Pathway: Destruction for the Sake of Construction. *Physiol. Rev.* 82, 373–428. doi:10.1152/physrev.00027.2001.

Graves, J. D., and Krebs, E. G. (1960). Protein phosphorylation and signal transduction. *Pharmacol. Ther.* 82, 111–21. doi:10.1016/S0163-7258(98)00056-4.

Gu, Y., and Innes, R. W. (2011). The KEEP ON GOING protein of Arabidopsis recruits the ENHANCED DISEASE RESISTANCE1 protein to trans-Golgi network/early endosome vesicles. *Plant Physiol.* 155, 1827–38. doi:10.1104/pp.110.171785.

Gu, Y., Rosenblatt, J., and Morgan, D. O. (1992). Cell cycle regulation of CDK2 activity by phosphorylation of Thr160 and Tyr15. *EMBO J.* 11, 3995–4005.

Hanson, A. D., and Roje, S. (2001). One -Carbon Metabolism In Higher Plants. *Annu. Rev. Plant Physiol.* 52, 119–137.

Hatfield, P. M., Gosink, M. M., Carpenter, T. B., and Vierstra, R. D. (1997). The ubiquitin-activating enzyme (E1) gene family in Arabidopsis thaliana. *Plant J.* 11, 213–226. doi:10.1046/j.1365-313X.1997.11020213.x.

Herman, P. P. L., Ramberg, H., Baack, R. R. D., Markwell, J., and Osterman, J. C. (2002). Formate dehydrogenase in Arabidopsis thaliana : overexpression and subcellular localization in lea v es. *Plant Sci.* 163, 1137–1145. doi:10.1016/S0168-9452(02)00326-6.

Hershko, A., Ciechanover, A., and Varshavsky, A. (1998). The ubiquitin system. *Nat. Med.*, 425–479. doi:10.1038/80384.

Hourton-Cabassa, C., Ambard-Bretteville, F., Moreau, F., Davy de Virville J, Rémy, R., and Francs-Small, C. (1998). Stress Induction of Mitochondrial Formate Dehydrogenase in Potato Leaves. *Plant Physiol.* 116, 627–35. Available at: http://www.pubmedcentral.nih.gov/articlerender.fcgi?artid=35120&tool=pmcentrez&rendertype=abstract.

Hunter, T. (2007). The Age of Crosstalk: Phosphorylation, Ubiquitination, and Beyond. *Mol. Cell* 28, 730–738. doi:10.1016/j.molcel.2007.11.019.

Ichimura, T., Yamamura, H., Sasamoto, K., Tominaga, Y., Taoka, M., Kakiuchi, K., et al. (2005). 14-3-3 Proteins modulate the expression of epithelial Na+ channels by phosphorylation-dependent interaction with Nedd4-2 ubiquitin ligase. *J. Biol. Chem.* 280, 13187–13194. doi:10.1074/jbc.M412884200.

Igamberdiev, A., Bykova, N. V., and Kleczkowski, L. (1999). Origins and metabolism of formate in higher plants. *Plant Physiol. Biochem.* 37, 503–513.

Jones, R., and Mansfield, T. (1970). Suppression of stomatal opening in leaves treated with abscisic acid. *J. Exp. Bot.* 21, 714–719. doi:10.1093/jxb/21.3.714.

Khoury, G., Baliban, R., and Floudas, C. (2011). Proteome-wide post-translational modification statistics: frequency analysis and curation of the swiss-prot database. *Sci. Rep.* 1, 1–5. doi:10.1038/srep00090.

Kim, D.-Y., Scalf, M., Smith, L. M., and Vierstra, R. D. (2013). Advanced proteomic analyses yield a deep catalog of ubiquitylation targets in Arabidopsis. *Plant Cell* 25, 1523–40. doi:10.1105/tpc.112.108613.

Komander, D., and Rape, M. (2012). The Ubiquitin Code. *Annu. Rev. Biochem.* 81, 203–229. doi:10.1146/annurev-biochem-060310-170328.

Kong, L., Cheng, J., Zhu, Y., Ding, Y., Meng, J., Chen, Z., et al. (2015). Degradation of the ABA co-receptor ABI1 by PUB12/13 U-box E3 ligases. *Nat. Commun.* 6, 8630. doi:10.1038/ncomms9630.

Kraft, E., Stone, S., Ma, L., Su, N., Gao, Y., Lau, O.-S., et al. (2005). Genome analysis and functional characterization of the E2 and RING-type E3 ligase ubiquitination enzymes of Arabidopsis. *Plant Physiol.* 139, 1597–1611. doi:10.1104/pp.105.067983.the.

Laemmli, U. K. (1970). Cleavage of Structural Proteins during the Assembly of the Head of Bacteriophage T4. *Nature* 227, 680–685.

Lecker, S. H. (2006). Protein Degradation by the Ubiquitin-Proteasome Pathway in Normal and Disease States. *J. Am. Soc. Nephrol.* 17, 1807–1819. doi:10.1681/ASN.2006010083.

Li, R., Bonham-Smith, P. C., and King, J. (2001). Molecular characterization and regulation of formate dehydrogenase in Arabidopsis thaliana. *Can. J. Bot. Can. Bot.* 79, 796–804. doi:10.1139/cjb-79-7-796.

Li, R., Moore, M., Bonham-Smith, P., and King, J. (2002). Overexpression of formate dehydrogenase in Arabidopsis thaliana resulted in plants tolerant to high concentrations of formate. *J. Plant Physiol.* 1076. Available at: http://www.sciencedirect.com/science/article/pii/S0176161704703260 [Accessed June 18, 2014].

Li, R., Moore, M., and King, J. (2003). Investigating the regulation of one-carbon metabolism in Arabidopsis thaliana. *Plant Cell Physiol.* 44, 233–241.

Liu, H., and Stone, S. (2010). Abscisic acid increases Arabidopsis ABI5 transcription factor levels by promoting KEG E3 ligase self-ubiquitination and proteasomal degradation. *Plant Cell* 22, 2630–41. doi:10.1105/tpc.110.076075.

Lyzenga, W. J., Liu, H., Schofield, A., Muise-Hennessey, A., and Stone, S. (2013). Arabidopsis CIPK26 interacts with KEG, components of the ABA signalling network and is degraded by the ubiquitin-proteasome system. *J. Exp. Bot.* 64, 2779–91. doi:10.1093/jxb/ert123.

Mazzucotelli, E., Belloni, S., Marone, D., De Leonardis, A., Guerra, D., Di Fonzo, N., et al. (2006). The e3 ubiquitin ligase gene family in plants: regulation by degradation. *Curr. Genomics* 7, 509–22. doi:10.2174/138920206779315728.

McWilliam, H., Li, W., Uludag, M., Squizzato, S., Park, Y. M., Buso, N., et al. (2013). Analysis Tool Web Services from the EMBL-EBI. *Nucleic Acids Res.* 41, 597–600. doi:10.1093/nar/gkt376.

Nishi, H., Hashimoto, K., and Panchenko, A. R. (2011). Phosphorylation in protein-protein binding: Effect on stability and function. *Structure* 19, 1807–1815. doi:10.1016/j.str.2011.09.021.

Oliver, D. J. (1981). Formate Oxidation and Oxygen Reduction by Leaf Mitochondria. *Plant Physiol.* 68, 703–705. doi:10.1104/pp.68.3.703.

Olson, B., Skavdahl, M., Ramberg, H., Osterman, J., and Markwell, J. (2000). Formate dehydrogenase in Arabidopsis thaliana: characterization and possible targeting to the chloroplast. *Plant Sci.* 159, 205–212. Available at: http://www.ncbi.nlm.nih.gov/pubmed/11074273.

Peters, J. M., Franke, W. W., and Kleinschmidt, J. A. (1994). Distinct 19 S and 20 S subcomplexes of the 26 S proteasome and their distribution in the nucleus and the cytoplasm. *J. Biol. Chem.* 269, 7709–7718.

Pickart, C. M. (2001). Mechanisms nderlying ubiquitination. *Annu. Rev. Biochem.* 70, 503–33. doi:10.1146/annurev.biochem.70.1.503.

Popov, V., and Lamzin, V. (1994). NAD+ dependent formate dehydrogenase. *Biochem. J.* 301, 625–643.

Roitinger, E., Hofer, M., Köcher, T., Pichler, P., Novatchkova, M., Yang, J., et al. (2015). MCP Papers in Press. Published on January 5, 2015 as Manuscript M114.040352 Quantitative Phosphoproteomics of the ATM and ATR dependent DNA damage response in. *Mol. Cell. Proteomics*, mcp.M114.040352. doi:10.1074/mcp.M114.040352.

Sedgwick, S. G., and Smerdon, S. J. (1999). The ankyrin repeat: a diversity of interactions on a common structural framework. *Trends Biochem. Sci.* 24, 311–6. Available at: http://www.ncbi.nlm.nih.gov/pubmed/10431175.

Shabek, N., and Ciechanover, A. (2010). Degradation of ubiquitin: The fate of the cellular reaper. *Cell Cycle* 9, 523–530. doi:10.4161/cc.9.3.11152.

Smalle, J., and Vierstra, R. D. (2004). The ubiquitin 26S proteasome proteolytic pathway. *Annu. Rev. Plant Biol.* 55, 555–90. doi:10.1146/annurev.arplant.55.031903.141801.

Stone, S. (2014). The role of ubiquitin and the 26S proteasome in plant abiotic stress signaling. *Front. Plant Sci.* 5, 135. doi:10.3389/fpls.2014.00135.

Stone, S., Hauksdóttir, H., and Troy, A. (2005). Functional Analysis of the RING-Type Ubiquitin Ligase Family of Arabidopsis. *Plant Physiol.* 137, 13–30. doi:10.1104/pp.104.052423.carrying.

Stone, S., Williams, L., Farmer, L., Vierstra, R., and Callis, J. (2006). KEEP ON GOING, a RING E3 ligase essential for Arabidopsis growth and development, is involved in abscisic acid signaling. *Plant Cell* 18, 3415–3428. doi:10.1105/tpc.106.046532.

Suzuki, K., Itai, R., Nakanishi, H., Nishizawa, N. K., Yoshimura, E., and Mori, S. (1998). Formate dehydrogenase, an enzyme of anaerobic metabolism, is induced by iron deficiency in barley roots. *Plant Physiol.* 116, 725–32. Available at: http://www.pubmedcentral.nih.gov/articlerender.fcgi?artid=35132&tool=pmcentrez&rendertype=abstract.

Swamy, P. M., and Smith, B. (1999). Role of abscisic acid in plant stress tolerance. *Curr. Sci.* 76, 1220–1227.

Thrower, J., Hoffman, L., Rechsteiner, M., and Pickart, C. M. (2000). Recognition of the polyubiquitin proteolytic signal. *EMBO J.* 19, 94–102. doi:10.1093/emboj/19.1.94.

Vierstra, R. D. (2003). The ubiquitin/26S proteasome pathway, the complex last chapter in the life of many plant proteins. *Trends Plant Sci.* 8, 135–142. doi:10.1016/S1360-1385(03)00014-1.

Vierstra, R. D. (2009). The ubiquitin–26S proteasome system at the nexus of plant biology. *Nat. Rev. Mol. Cell Biol.* 10, 385–397. doi:10.1038/nrm2688.

Wang, F., Zhu, D., Huang, X., Li, S., Gong, Y., Yao, Q., et al. (2009). Biochemical insights on degradation of Arabidopsis DELLA proteins gained from a cell-free assay system. *Plant Cell* 21, 2378–2390. doi:10.1105/tpc.108.065433.

Wang, Y. H., and Irving, H. R. (2011). Developing a model of plant hormone interactions. *Plant Signal. Behav.* 6, 494–500. doi:10.4161/psb.6.4.14558.

Welch, B. L. (1947). The Generalization of "Student"S' Problem When Several Different Population Varlances Are Involved. *Biometrika* 34, 28–35. doi:10.1093/biomet/34.1-2.28.

Xue, L., Wang, P., Wang, L., Renzi, E., Radivojac, P., Tang, H., et al. (2013). Quantitative measurement of phosphoproteome response to osmotic stress in Arabidopsis based on Library-Assisted eXtracted Ion Chromatogram (LAXIC). *Mol. Cell. Proteomics* 53, 1–39. doi:10.1017/CBO9781107415324.004.

Zheng, N., Wang, P., Jeffrey, P. D., and Pavletich, N. P. (2000). Structure of a c-Cbl-UbcH7 complex: RING domain function in ubiquitin-protein ligases. *Cell* 102, 533–9. Available at: http://www.ncbi.nlm.nih.gov/pubmed/10966114.

Zuin, A., Isasa, M., and Crosas, B. (2014). Ubiquitin Signaling: Extreme Conservation as a Source of Diversity. *Cells* 3, 690–701. doi:10.3390/cells3030690.

APPENDIX

The following supplemental figures (S1-S8) are replicates, expanded time points or images of the representative data displayed in the results section.

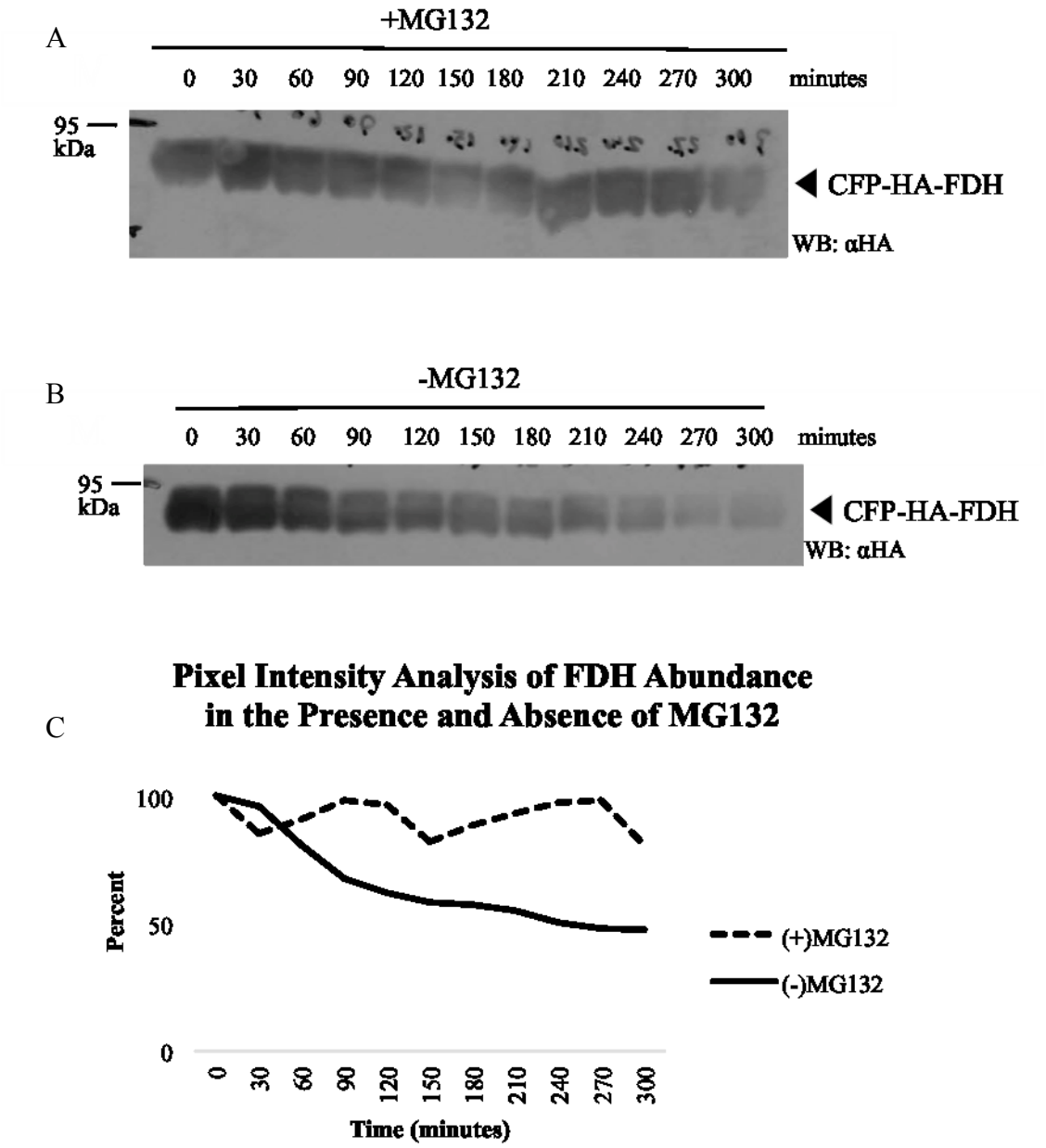

Supplemental Figure S-1: FDH is Degraded by the 26S Proteasome. Replicate of cell free degradation assay showing A) that when incubated with the 26S proteasome inhibitor, MG132, CFP-HA-FDH remains more stable than B) CFP-HA-FDH incubated with an active 26S proteasome. C) Pixel intensity analysis comparing the degradation of CFP-HA-FDH in the absence or presence of MG132. Ponceau S shows equal protein loading.

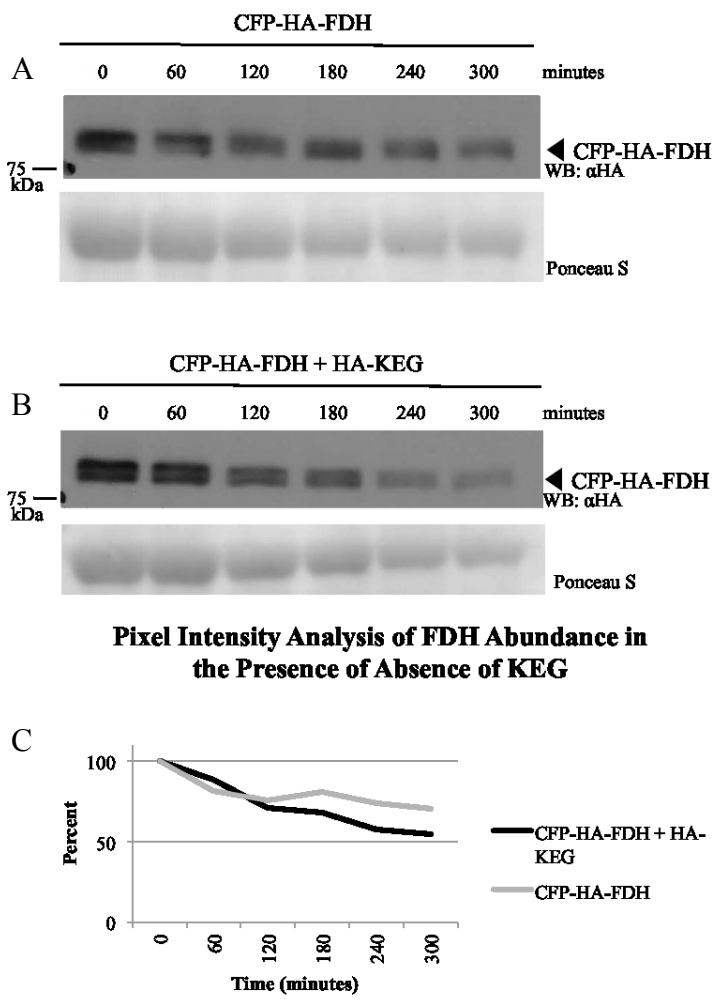

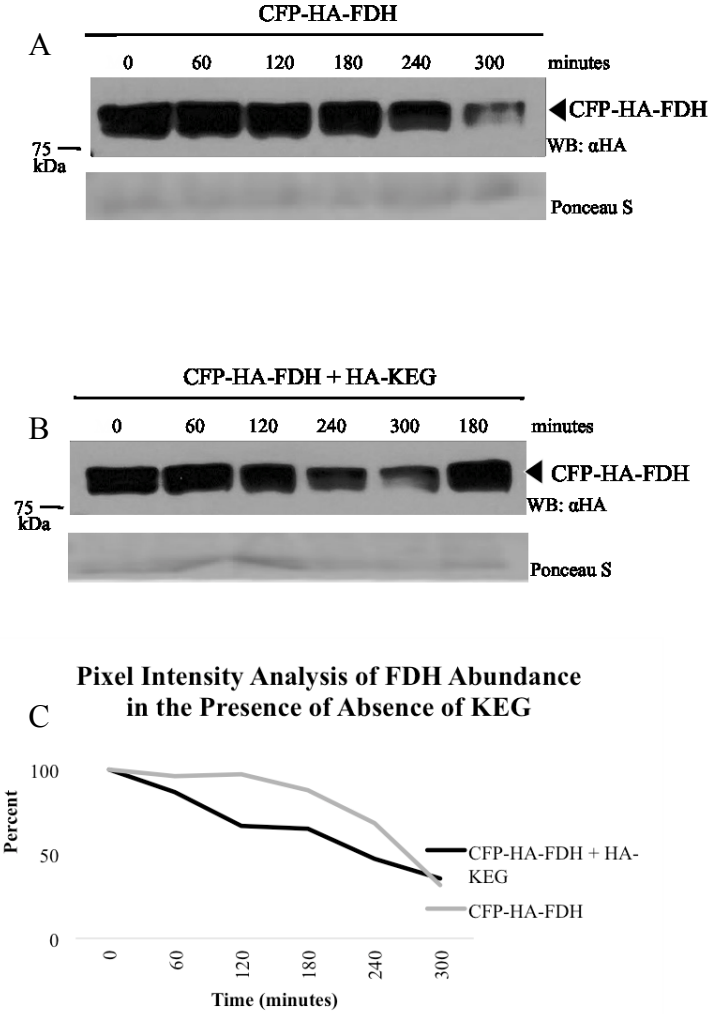

Supplemental Figure S-2: FDH Degradation is Dependent on KEG. A) Replicates of cell free degradation assay depicting the abundance of CFP-HA-FDH over time when it is expressed on it's own or B) co-expressed with HA-KEG. C) Pixel intensity analysis showing that the degradation of CFP-HA-FDH is faster when co-expressed with HA-KEG. Ponceau S demonstrations that protein loading was equal

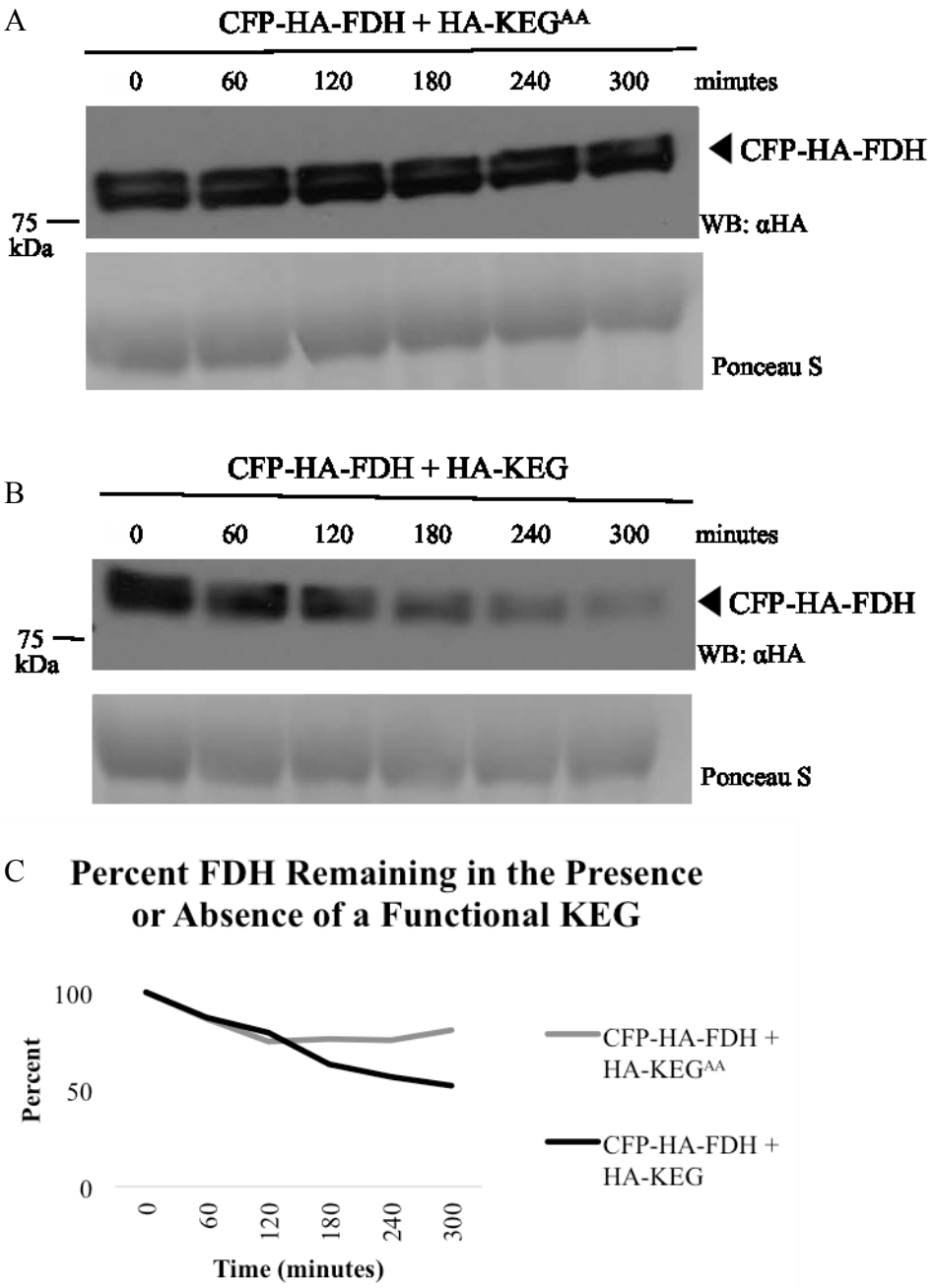

Supplemental Figure S-3: FDH Degradation Requires A Functional RING Domain. A) Replicate of cell free degradation assay showing CFP-HA-FDH abundance over time when co-expressed with the RING mutated, HA-KEG^{AA} or B) co-expressed with HA-KEG, possessing a functional RING domain. C) Pixel intensity analysis shows that when CFP-HA-FDH is co-expressed with HA-KEG that it is degraded faster than when co-expressed with the RING mutated HA-KEG^{AA}. Ponceau S shows that the protein loading is equal between lanes.

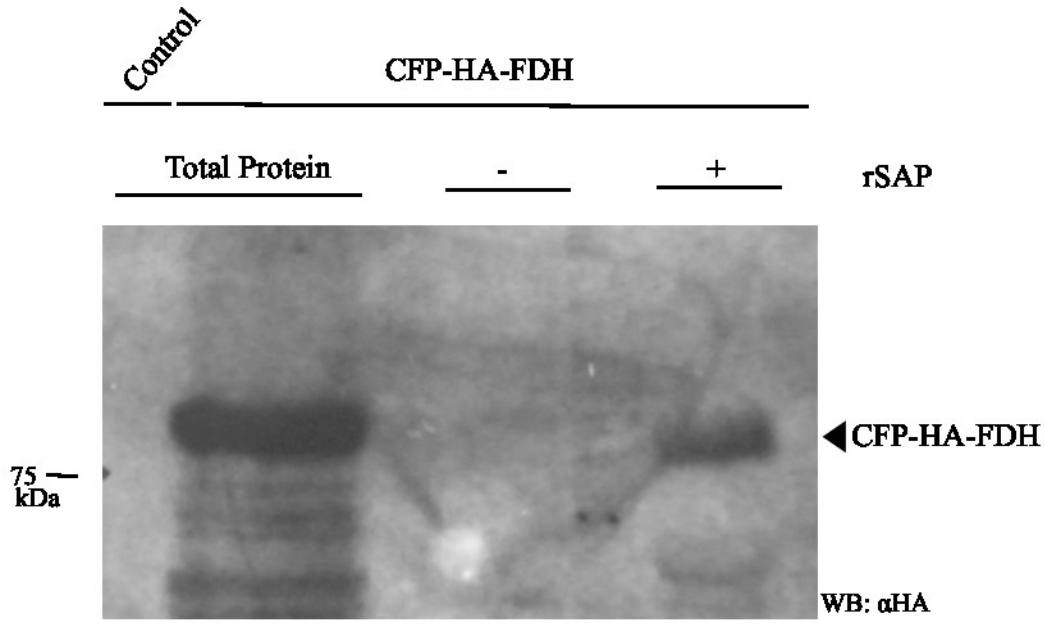

Supplemental Figure S-4: Dephosphorylation Assay. A) Replicate of total protein extracts containing CF-HA-FDH incubated with an alkaline phosphatase (rSAP) ran at a lower molecular weight than the un-incubated sample.

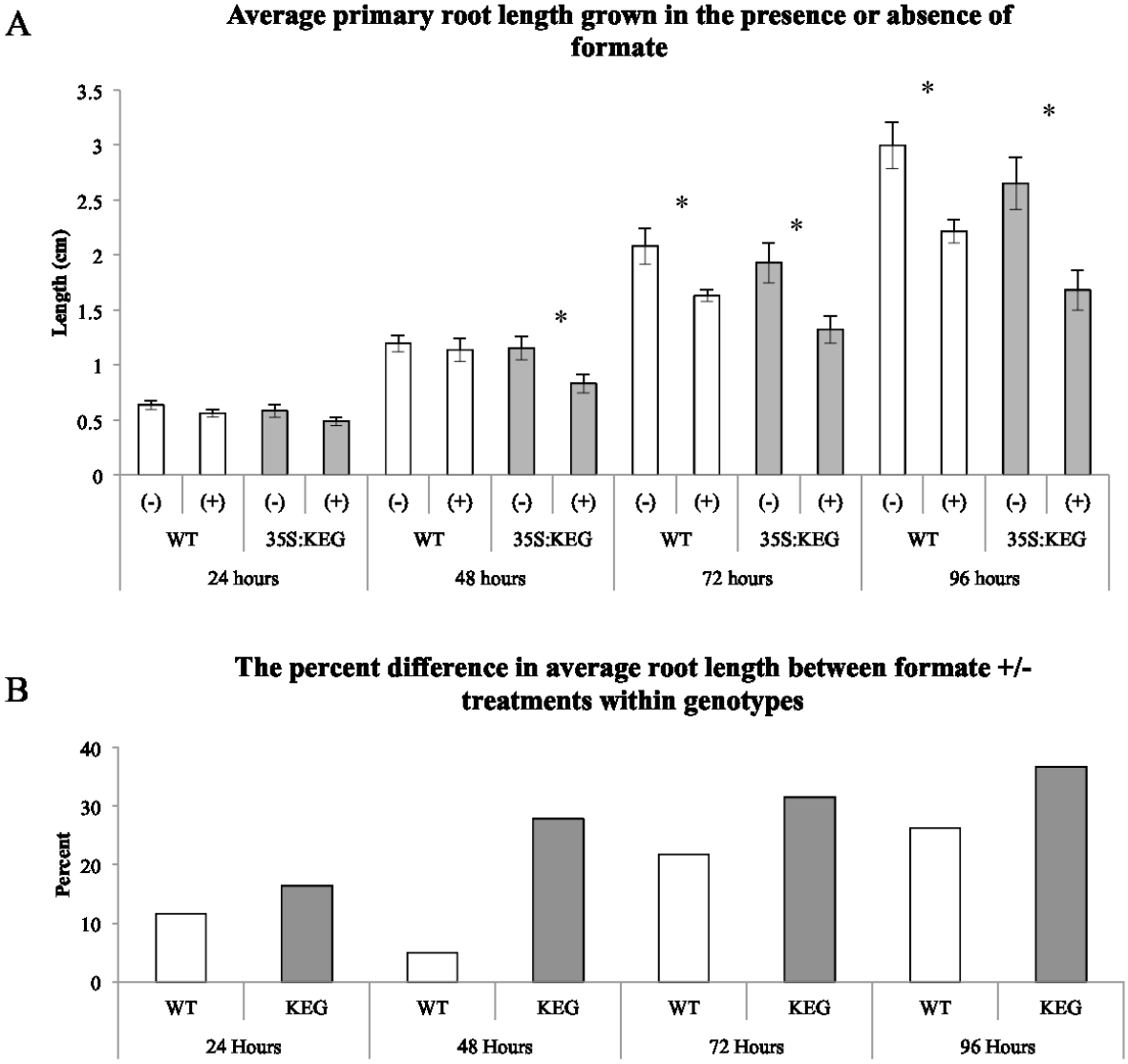

Supplemental Figure S-5: Formate Sensitivity Analysis. A) Formate Sensitivity Analysis. Average primary root length of wild-type (WT) and transgenic Arabidopsis constitutively expressing KEG (KEG O/E) on standard ½ murashige and skoog (MS) media in the presence (+) or absence (-) of formate after at 24 hour time points. Root length was shorter for KEG O/E in the presence of formate, indicating that they are more sensitive to the exogenous addition of formate. Each treatment group consisted of 12 individual seedlings. Bars represent standard error. Asterisks indicate significant difference between means. B) The percent difference in root length of plants grown in the presence or absence of formate, within genotypes. KEG O/E plants consistently have a higher percentage difference in their root length, indicating inhibition of primary root growth is stronger in KEG plants.

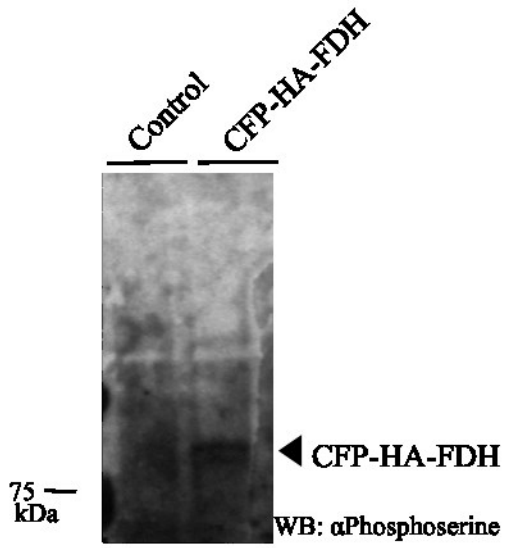

Supplemental Figure S-6: FDH Is Phosphorylated *In Planta*. Replicate of Immunoprecipitated total protein extracts containing CFP-HA-FDH were probed with a phosphoserine specific antibody and identified CFP-HA-FDH as a phosphorylated protein.

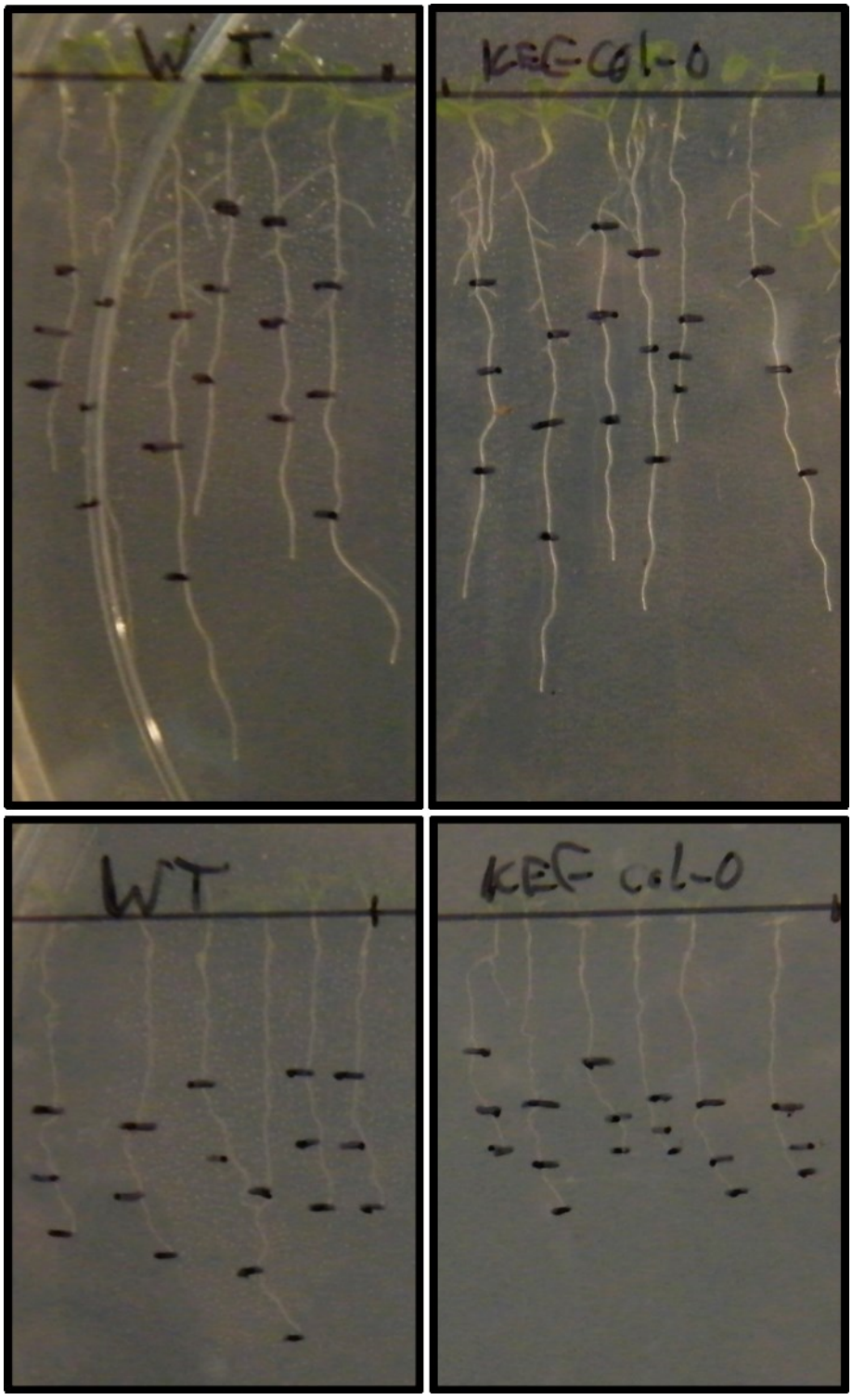

Supplemental Figure S-7: Image of Root Growth. Photograph of wild type (WT) and KEG over expressers (KEG col-0) after 72 hours of growth in the presence or absence of formate. Top two panels show WT and KEG over expressers grown on normal ½ Mushiage and Skoog (MS) medium. Bottom two panels show WT and KEG over expressers grown on ½ MS medium supplemented with formate. Black tick marks indicate the point of transfer – 0 hours, 24 hours, and 48 hours.

Supplemental Table S-8: Post-translational Modifiction Prediction Score. Predicted ubiquitination (Chen et al., 2013a) and phosphorylation (Blom et al., 1999) sites. Ubiquitinated lysine (K) residue cut off score was set at 0.7. Phosphorylated serine (S), threonine (T) and tyrosine (Y) residue cut off score was set at a default of 0.5 stringency.

Residue	Prediction Score	Post-translational Modification
K44	0.819	Ubiquitination
K51	0.821	Ubiquitination
K121	0.732	Ubiquitination
K198	0.877	Ubiquitination
K217	0.756	Ubiquitination
K273	0.818	Ubiquitination
K281	0.930	Ubiquitination
K355	0.737	Ubiquitination
K363	0.856	Ubiquitination
S15	0.985	Phosphorylation
S16	0.455	Phosphorylation
S17	0.828	Phosphorylation
S18	0.814	Phosphorylation
S20	0.992	Phosphorylation
S31	0.996	Phosphorylation
S35	0.889	Phosphorylation
S155	0.958	Phosphorylation
T10	0.517	Phosphorylation
T144	0.559	Phosphorylation
T264	0.695	Phosphorylation
T336	0.527	Phosphorylation
T342	0.502	Phosphorylation
T354	0.856	Phosphorylation
Y48	0.854	Phosphorylation
Y108	0.866	Phosphorylation
Y225	0.667	Phosphorylation
Y372	0.776	Phosphorylation